

Title: Cosmology from the SDSS

Speakers: Will Percival

Series: Cosmology & Gravitation

Date: July 28, 2020 - 11:00 AM

URL: <http://pirsa.org/20070028>

Abstract: On Monday July 20th, we announced the final results from extended Baryon Oscillation Spectroscopic Survey (eBOSS), the last large-scale structure galaxy survey to be undertaken within the umbrella of the Sloan Digital Sky Survey (SDSS). This marks the culmination of 20 years of galaxy surveys undertaken using the Sloan Foundation Telescope. In this seminar I will summarise the measurements presented in the 23 scientific papers that were released last Monday, and present the impact of the measurements from eBOSS and previous SDSS galaxy surveys on the development of the standard cosmological model.

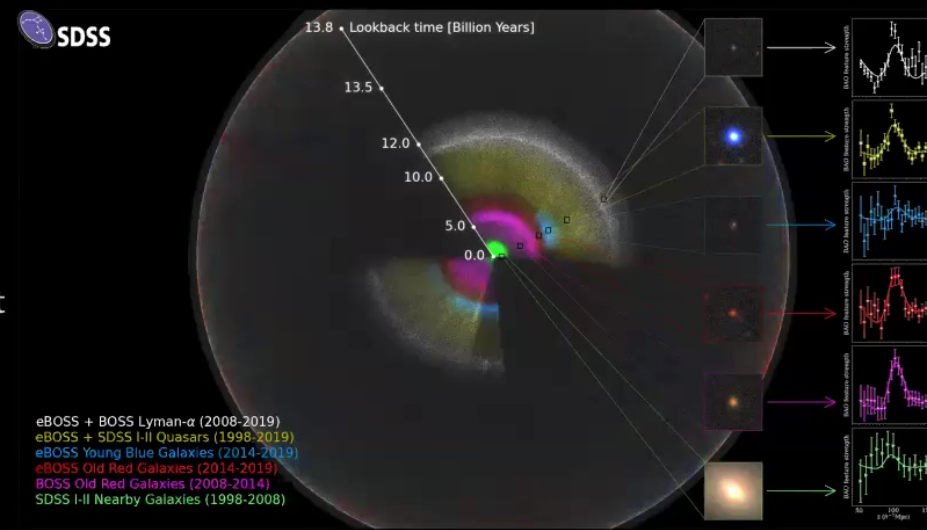
Final Cosmology from SDSS redshift surveys



Will Percival

Will Percival
Waterloo Centre for
Astrophysics
University of Waterloo /
Perimeter Institute

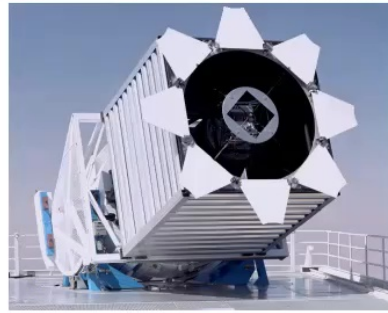
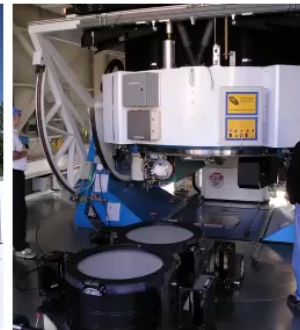
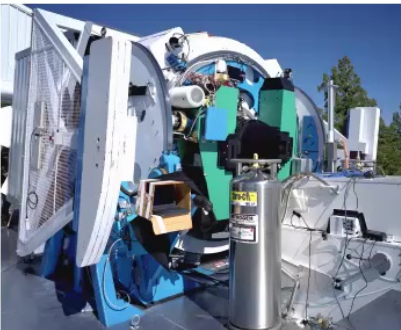
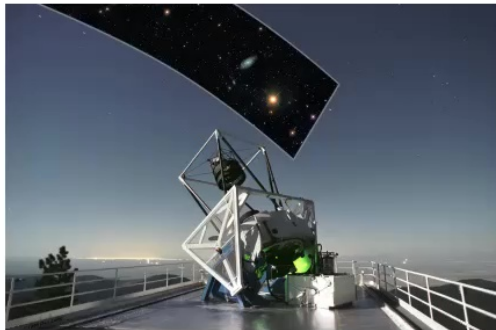
eBOSS Survey Scientist



WATERLOO CENTRE FOR
ASTROPHYSICS
UNIVERSITY OF WATERLOO



The Sloan Foundation Telescope 1998-2020



WATERLOO CENTRE FOR
+ ASTRO +
PHYSICS
UNIVERSITY OF WATERLOO

The SDSS large-scale structure galaxy surveys

- **1999-2009** The SDSS-I and -II gave us the Main Galaxy Sample (out to $z < 0.2$), and some LRGs subsequently subsumed into later surveys
- **2009-2014** SDSS-III included the BOSS experiment which observed luminous (mainly red) galaxies, and quasars for Ly- α forest measurements
- **2014-2019** SDSS-IV included the eBOSS experiment, which observed
 - Luminous red galaxies (LRG)
 - Emission line galaxies (ELG)
 - Quasars used as direct tracers
 - Quasars for Ly- α forest measurements
- Baryon Acoustic Oscillations (BAO) were observed in each sample. The aggregate precision of the expansion history measurements is 0.70% at redshifts $z < 1$ and 1.19% at redshifts $z > 1$,
- The aggregate precision of redshift space distortions (RSD) based growth measurements is 4.78% over the redshift interval $0 < z < 1.5$.
- With this redshift coverage and sensitivity, the SDSS experiment is unparalleled in its ability to explore models of cosmology.



The SDSS large-scale structure galaxy samples



Will Percival

Parameter	Main Galaxy Sample (MGS)	BOSS Galaxy	BOSS Galaxy	eBOSS LRG	eBOSS ELG	eBOSS Quasar	Ly α -Ly α	Ly α -Quasar
Imaging, Target Selection, and Spectroscopic Properties of Each Sample								
Imaging for Target Selection	SDSS	SDSS	SDSS	SDSS + WISE	DECaLS	SDSS + WISE	SDSS + WISE + MISC	SDSS + WISE + MISC
Target Selection	g,r	g,r,i	g,r,i	g,r,i,z,W1	g,r,z	u,g,r,i,z,W1,W2	misc	misc
Spectroscopic Program	SDSS-I and -II	BOSS	BOSS	BOSS and eBOSS	eBOSS	primarily eBOSS	BOSS and eBOSS	BOSS and eBOSS
redshift range	0.07 < z < 0.20	0.2 < z < 0.5	0.4 < z < 0.6	0.6 < z < 1.0	0.6 < z < 1.1	0.8 < z < 2.2	z > 2.1	z > 1.77
Number of Tracers	63,163	604,001	686,370	377,458	173,736	343,708	210,005	341,468
Effective Redshift	0.15	0.38	0.51	0.70	0.85	1.48	2.33	2.33
Effective Volume (Gpc^3)	0.24	3.7	4.2	2.7	0.6	0.6		
Clustering Catalog Documentation	Ross et al. (2020)	Reid et al. (2016)	Reid et al. (2016)	Ross et al. (2020)	Raichoor et al. (2020)	Ross et al. (2020) , Lyke et al. (2020)	du Mas des Bourboux et al. (2020) , Lyke et al. (2020)	du Mas des Bourboux et al. (2020) , Lyke et al. (2020)
N-body and Mock Catalogs		Kitaura et al. (2016)	Kitaura et al. (2016)	Zhao et al. (2020) , Rossi et al. (2020)	Zhao et al. (2020) , Lin et al. (2020) , Alam et al. (2020)	Zhao et al. (2020) , Smith et al. (2020)	Farr et al. (2020)	Farr et al. (2020)

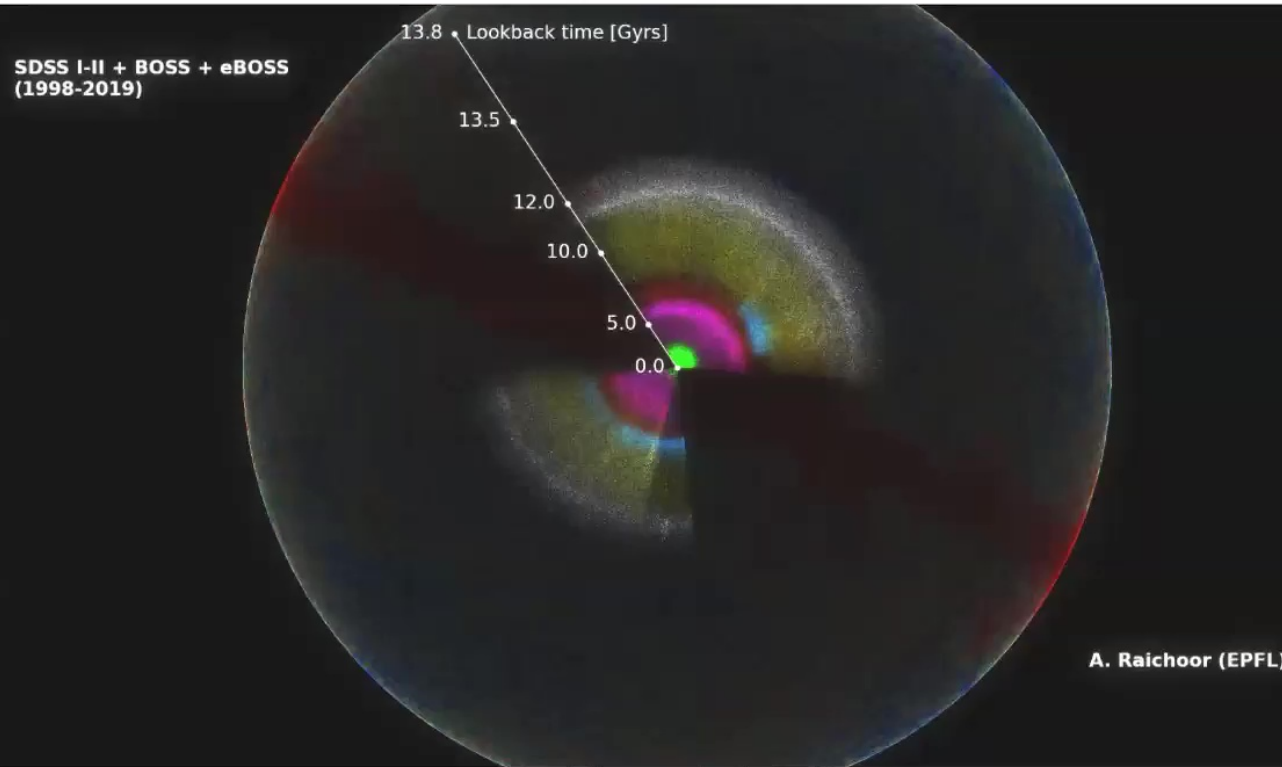
From <https://www.sdss.org/science/final-bao-and-rsd-measurements/>



The SDSS galaxy surveys

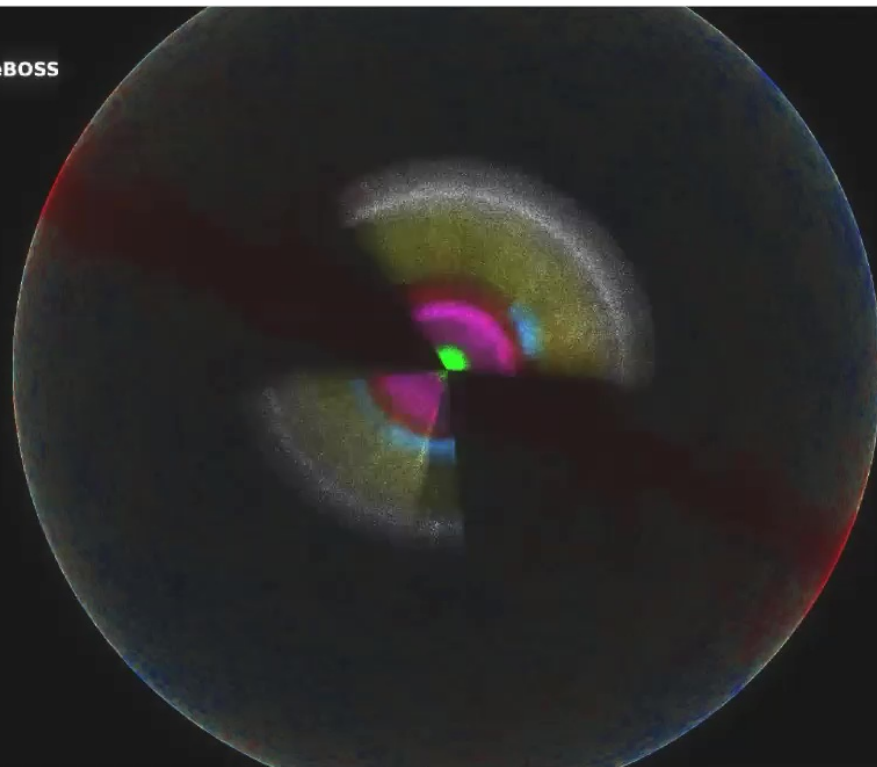


Will Percival



The SDSS galaxy surveys

SDSS I-II + BOSS + eBOSS
(1998-2019)

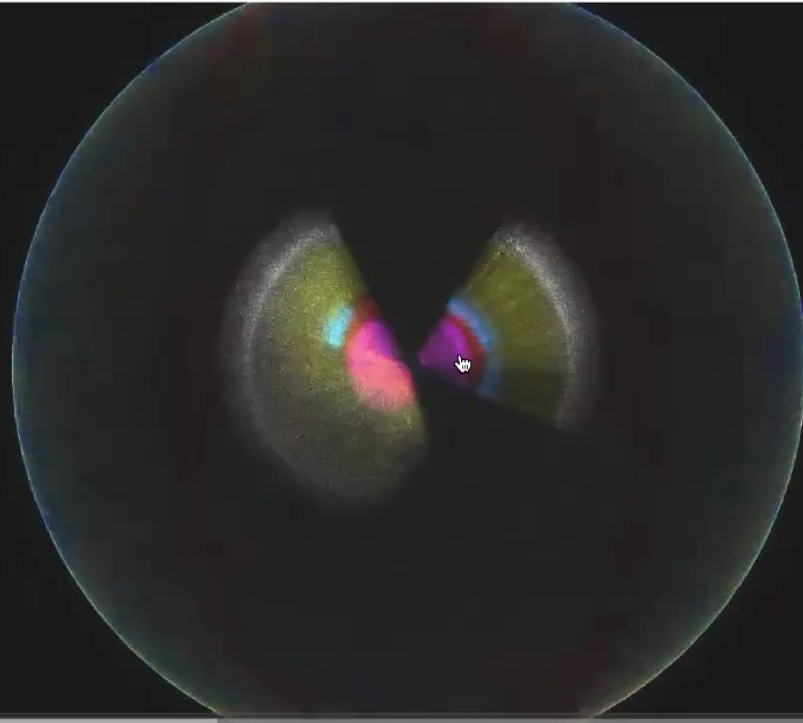


Will Percival

The SDSS galaxy surveys



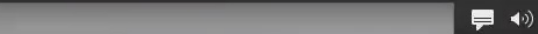
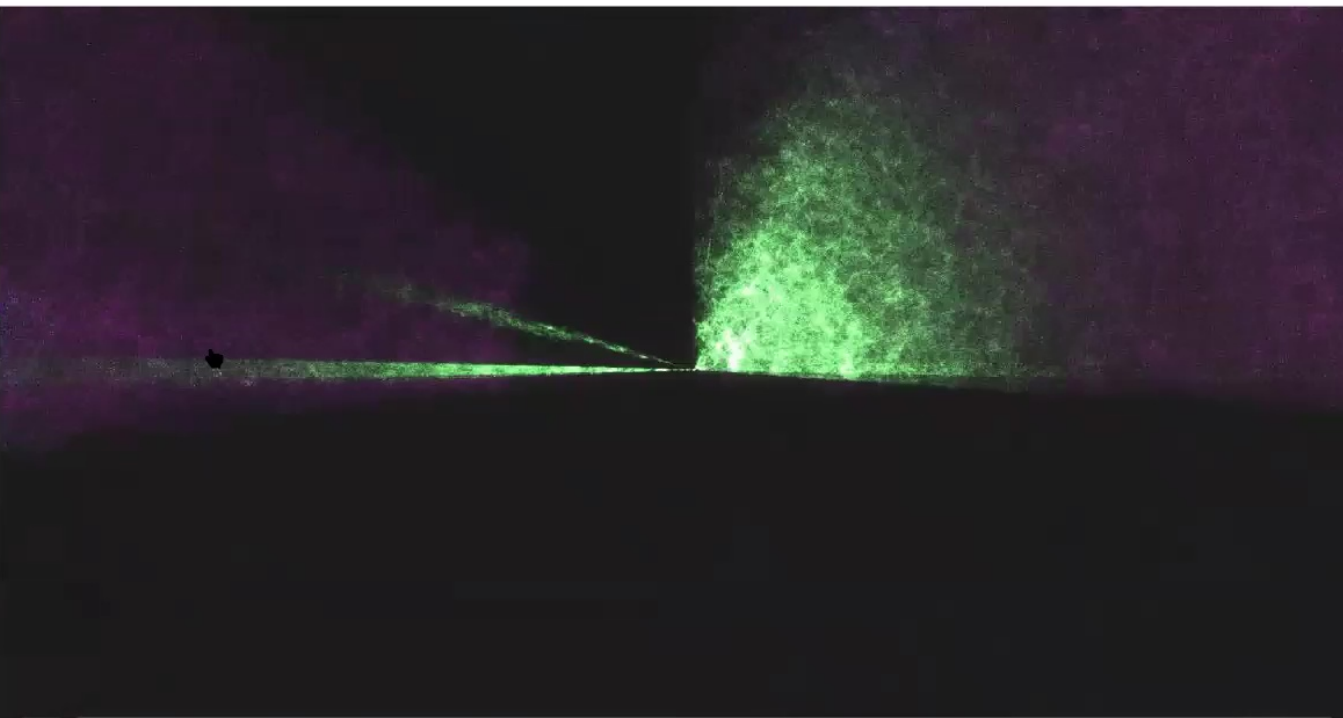
Will Percival



The SDSS galaxy surveys



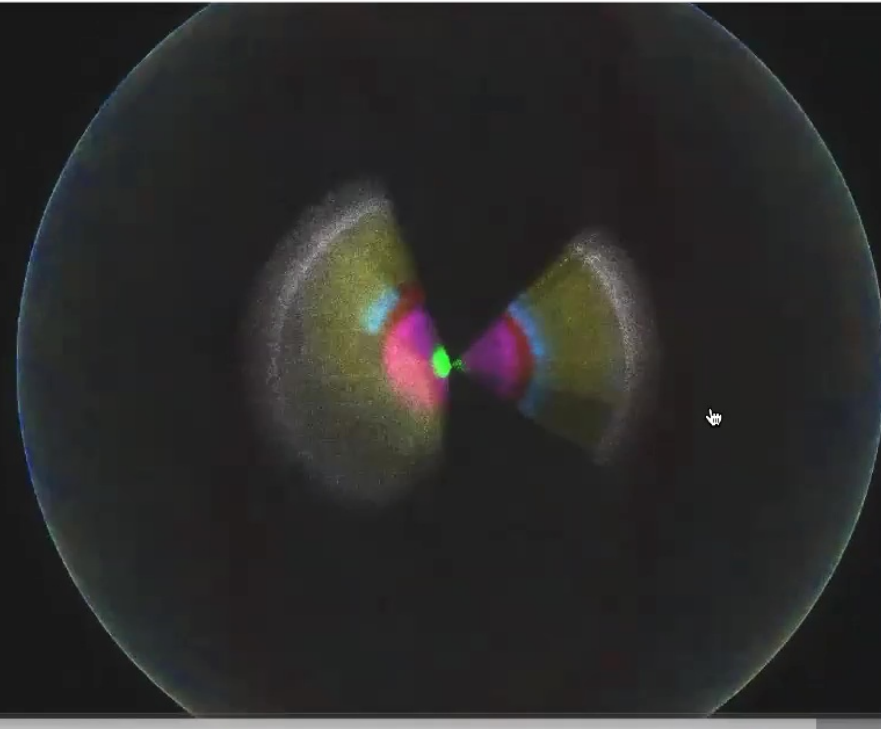
Will Percival



The SDSS galaxy surveys



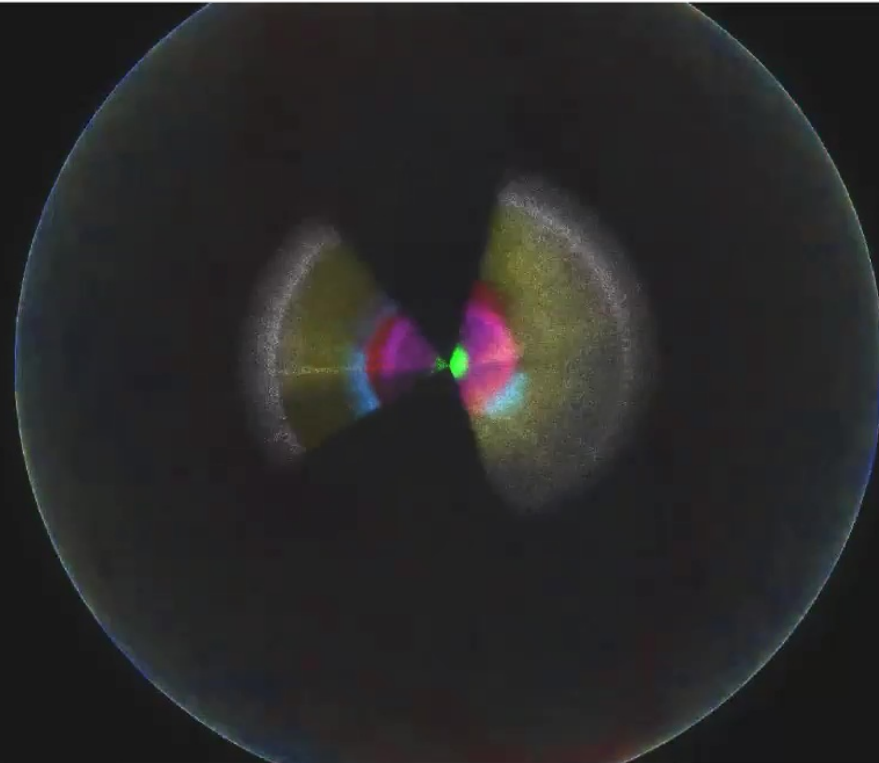
Will Percival



The SDSS galaxy surveys



Will Percival



eBOSS – the end of an era

- SDSS-V will not perform a LSS redshift survey
- eBOSS announcement last week was last using a galaxy redshift survey from SDSS
- Out with a bang! – 23 papers on the archive last Monday
- 4 promotional videos (2 with ~300k hits)
- press releases (with local variations around the world)
- Many articles in the news, including some that were accurate and well written!
- The end of an era ...
- This seminar – hastily put together review of eBOSS and those 23 papers.



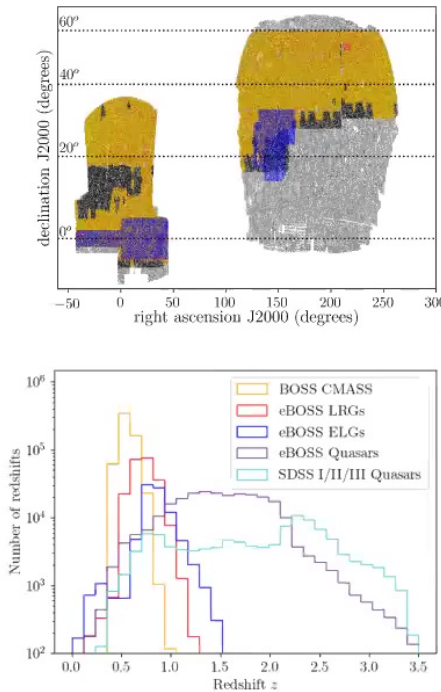


Will Percival

The eBOSS catalogs and tests

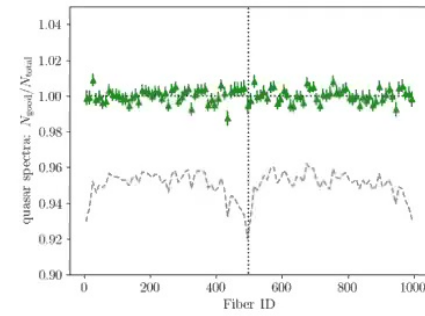


LRG & QSO clustering catalogs



Ross et al. (2020), arXiv:2007.09000

Turned the raw data into well-understood catalogs of objects and their expected density



Quasar redshift efficiency versus fiber – before and after correction

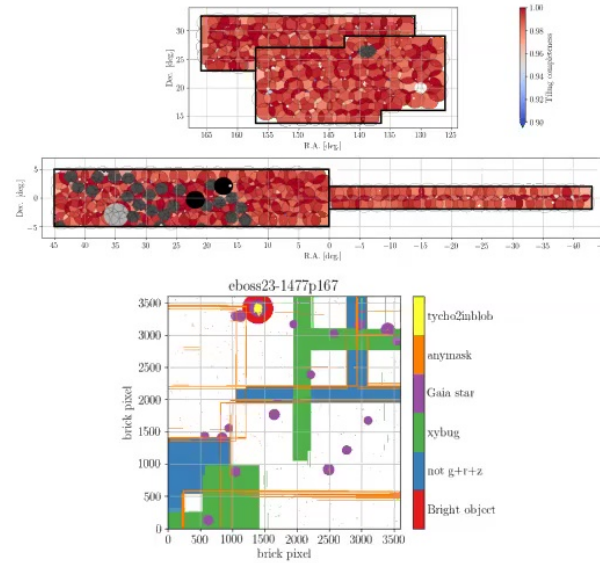
Results of LRG target spectroscopic observations

	SGC	NGC	Total
N_{eff}	87,607	134,695	222,302
$N_{z,\text{tot}}$	82,607	127,287	209,894
N_{zfail}	2,205	3,019	5,224
N_{cp}	3,436	4,950	8,386
N_{QSO}	1,254	1,635	2,889
N_{star}	10,749	10,017	20,766
after $C_{\text{eBOSS}} > 0.5, C_z > 0.5$ cuts:			
N_{eff}	86,511	133,540	220,051
$N_{z,\text{tot}}$	81,600	126,230	207,830
$N_{\text{eff}}, 0.6 < z < 1.0$	71,427	113,868	185,295
$N_{z,\text{tot}}, 0.6 < z < 1.0$	67,316	107,500	174,816
Area post-veto (deg^2)	1,676	2,566	4,242
Weighted area post-veto (deg^2)	1,627	2,476	4,103

Will Percival

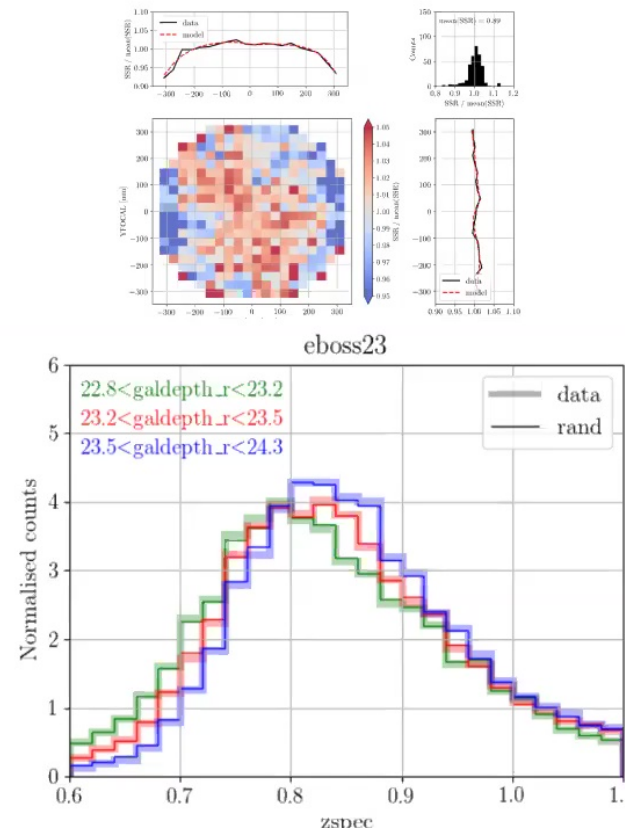


ELG clustering catalog

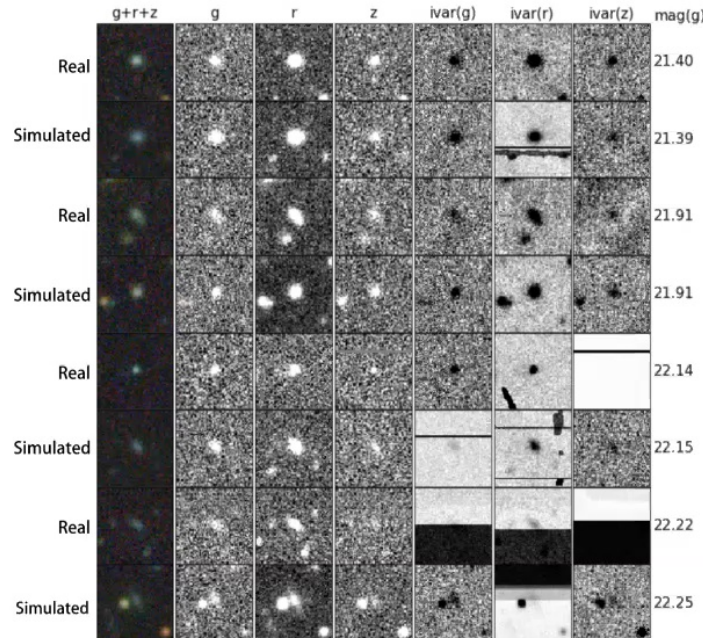


Turned the raw data into well-understood catalogs of objects and their expected density

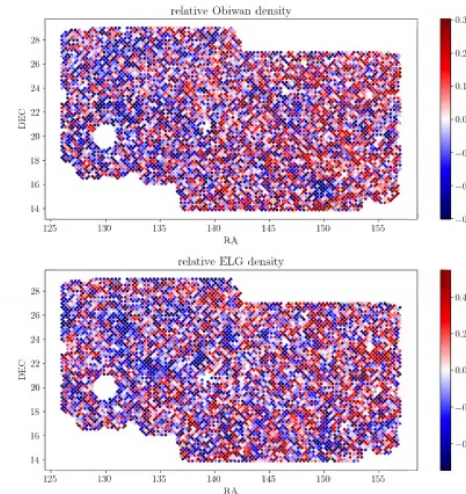
Raichoor et al. (2020), arXiv:2007.09007



Testing ELG target selection



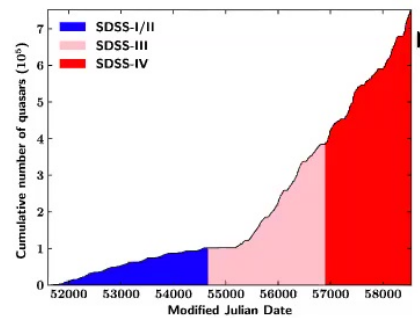
Used software called Obiwan to inject fake ELGs into the imaging data used for targeting and checked for large-scale systematics



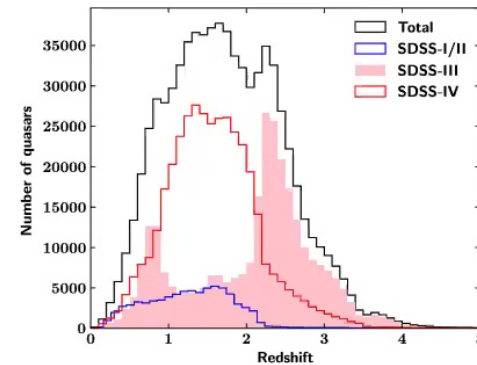
Kong et al. (2020), arXiv:2007.08992



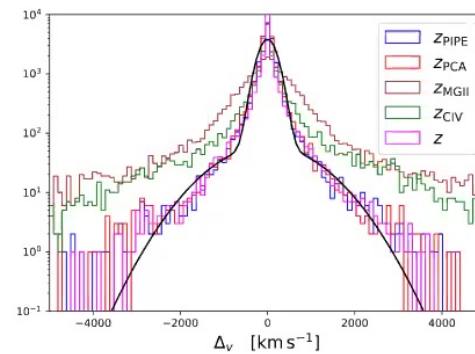
Quasar catalog



eBOSS primarily filled in the gap $1 < z < 2$, between low-redshift quasars and Ly- α quasars at high redshift



Tradition in SDSS to release a catalogue of all quasars observed, not just those whose expected clustering can be understood (the large-scale structure catalog)



Redshift measurement for quasars is more complicated than other objects due to outflows

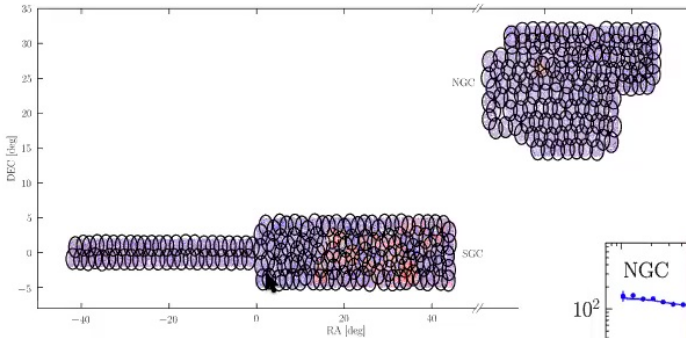


Lyke et al. (2020), arXiv:2007.09001

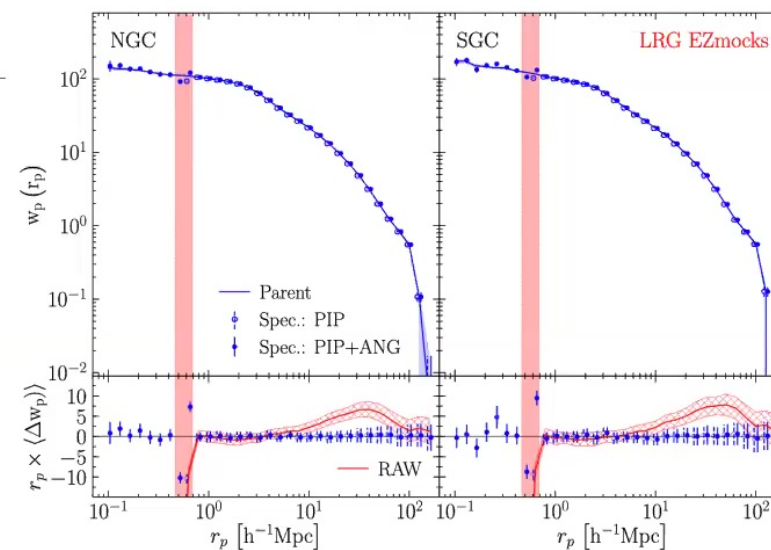
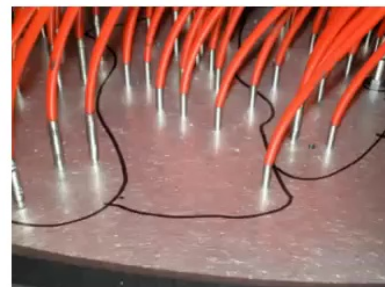


Will Percival

Dealing with fiber collisions



Created weights for each pair in the LRG, ELG and QSO catalogues to correct for fiber collisions and get the correct small-scale clustering



Mohammad et al. (2020), arXiv:2007.09005



Will Percival



Will Percival

The eBOSS mock catalogs

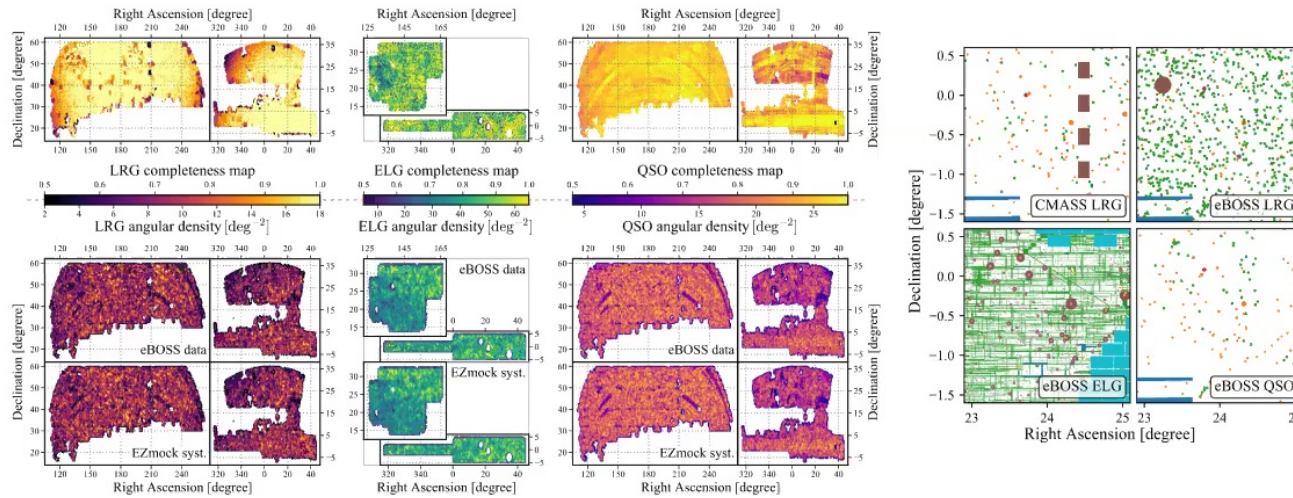


ELG-LRG-QSO approximate mocks



Will Percival

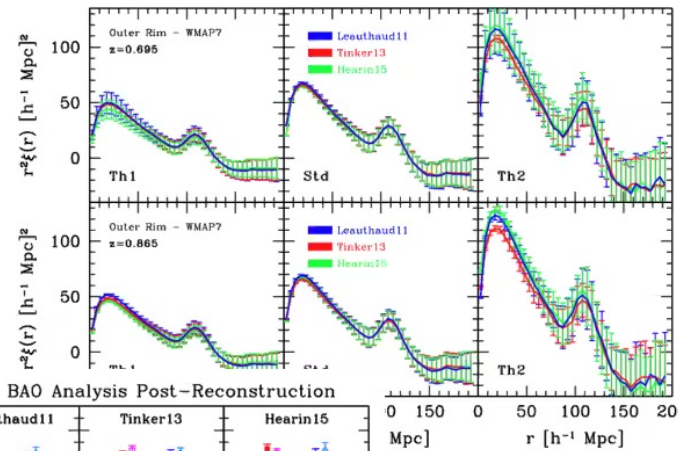
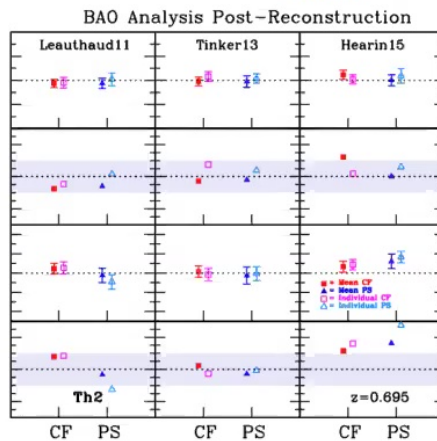
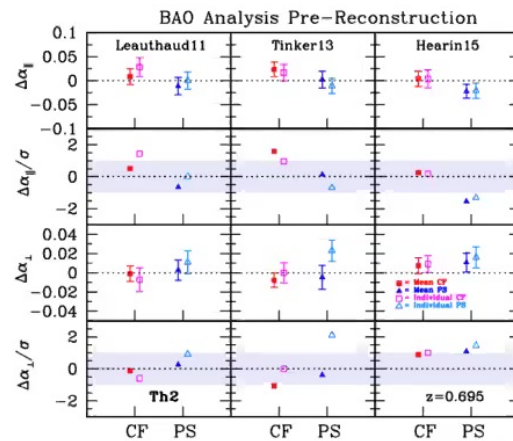
Created 1000 perturbation-theory based mocks, samples by each galaxy type, and turned into overlapping mock surveys



Zhao et al. (2020), arXiv:2007.08997

LRG mock challenge

Carried out internal mock challenge, where groups fit mock samples and try to recover unknown cosmological parameters – this analysis focussed particularly on the effect of small scales through the HOD used to populate the Outer Rim simulation.

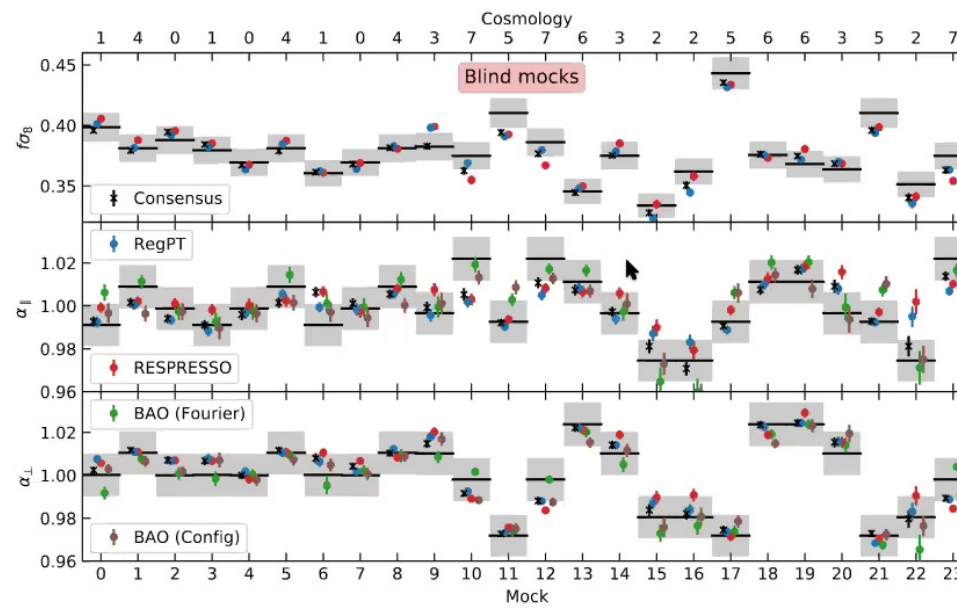


Rossi et al. (2020), arXiv:2007.09002



QSO mock challenge

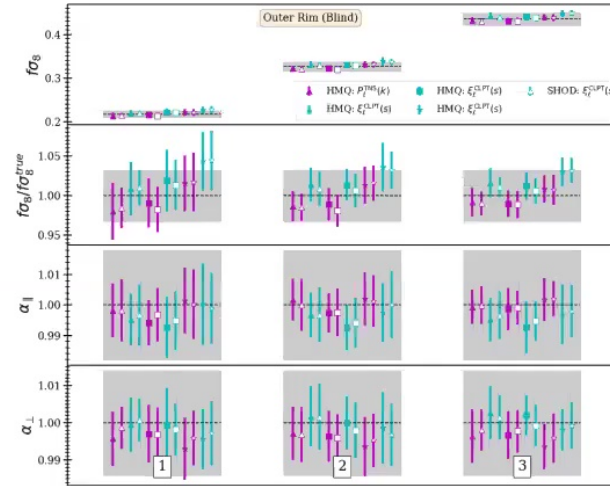
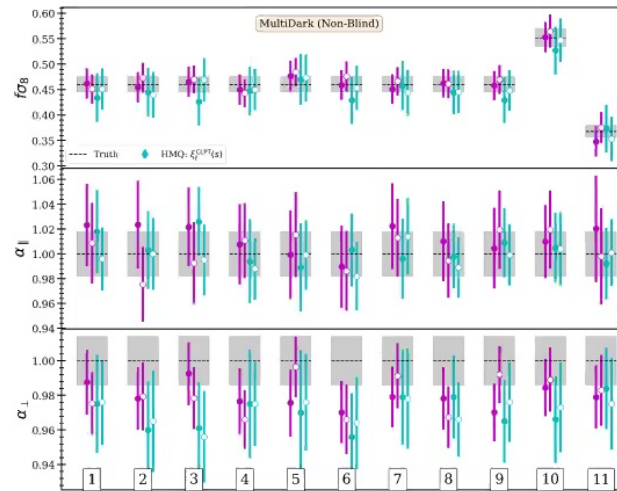
Blind tests on the recovery of cosmological parameters using QSO mocks with different cosmologies and HOD



Smith et al. (2020), arXiv:2007.09003

ELG mock challenge

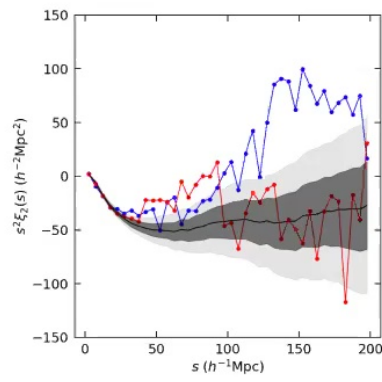
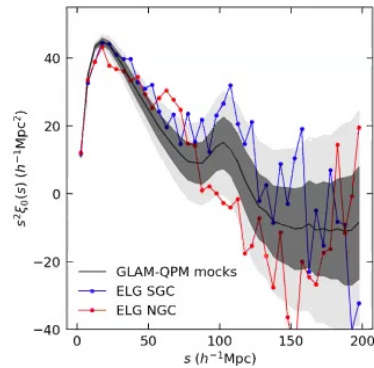
Blind tests on the recovery of cosmological parameters using ELG mocks with different cosmologies and HOD



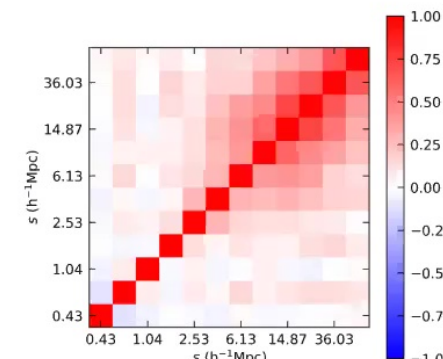
Alam et al. (2020), arXiv:2007.09004



ELG GLAM-QPM mocks



Ran 200 large GaLaxy Mocks (GLAM) N-body simulations, and placed haloes with a local density matching algorithm. Galaxies placed using Gaussian HOD. Used to test ELG modelling on small scales.



Lin et al. (2020), arXiv:2007.08996



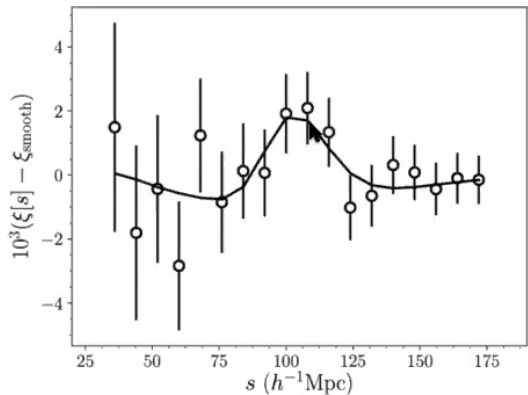


Will Percival

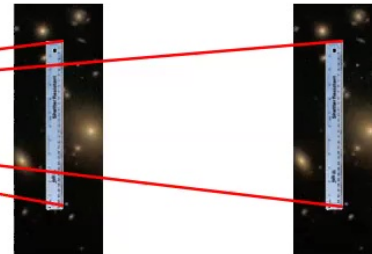
Baryon Acoustic Oscillations



BAO as an absolute ruler



eBOSS DR14 quasars at $z=1.52$
Ata et al. 2017; arXiv:1705.06373



Radial direction

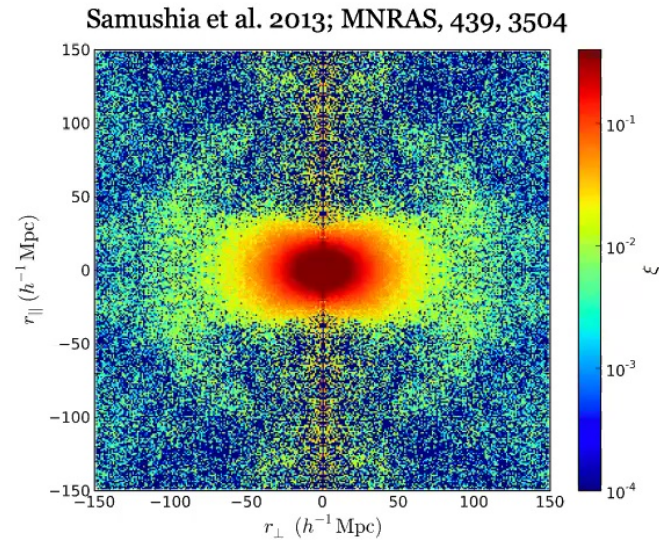
$$\alpha_{\parallel} \propto H(z)r_d$$

Angular direction

$$\alpha_{\perp} \propto \frac{D_A(z)}{r_d}$$



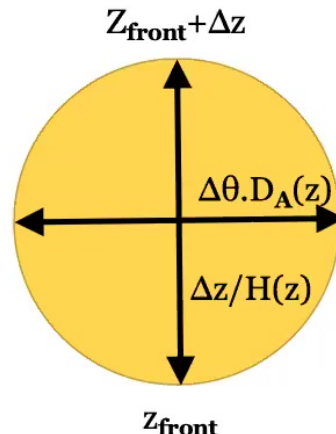
Relative BAO: position vs line-of-sight



$$\frac{\alpha_{\parallel}}{\alpha_{\perp}} \propto H(z) D_A(z)$$

Future Galaxy Surveys

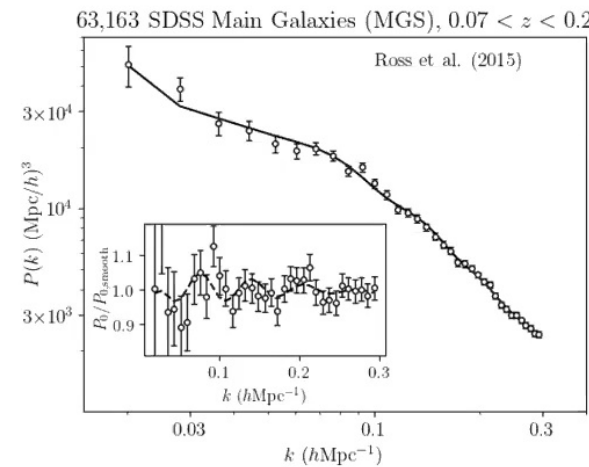
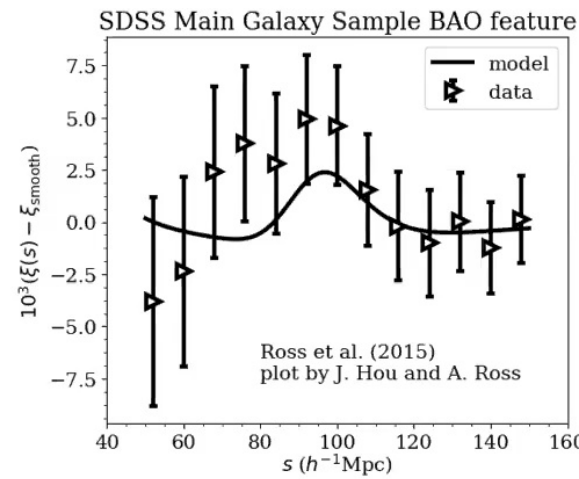
The Alcock-Paczynski effect



STANDARD SHAPE
[Minimum scale – cosmological expansion can still be recovered]



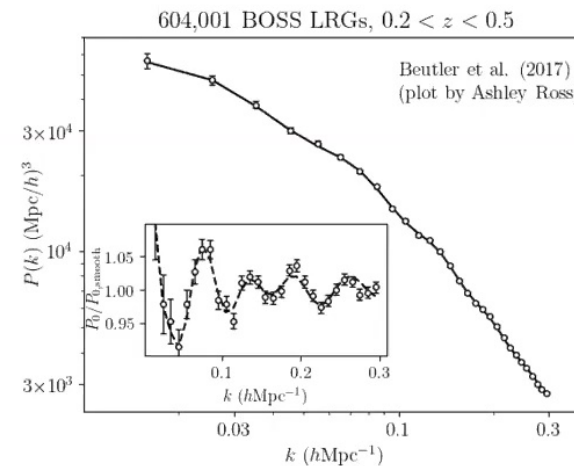
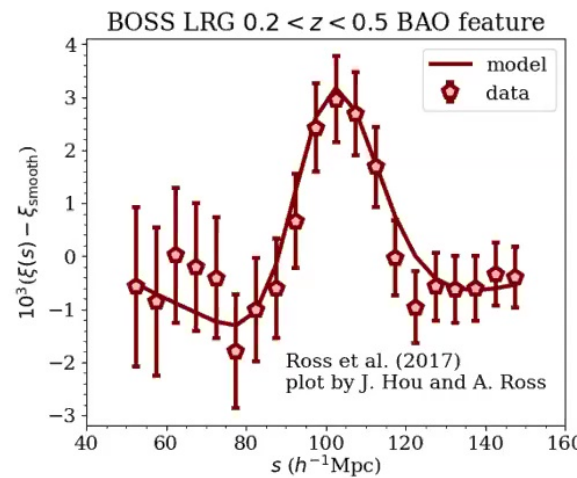
BAO from SDSS Main Galaxy Sample ($0.07 < z < 0.2$)



Ross et al. (2015), MNRAS 449, 835



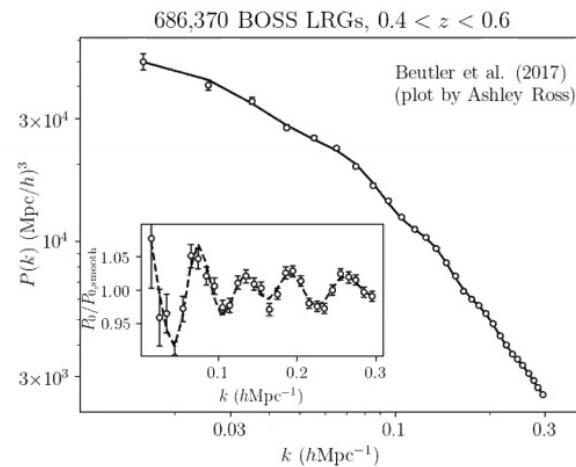
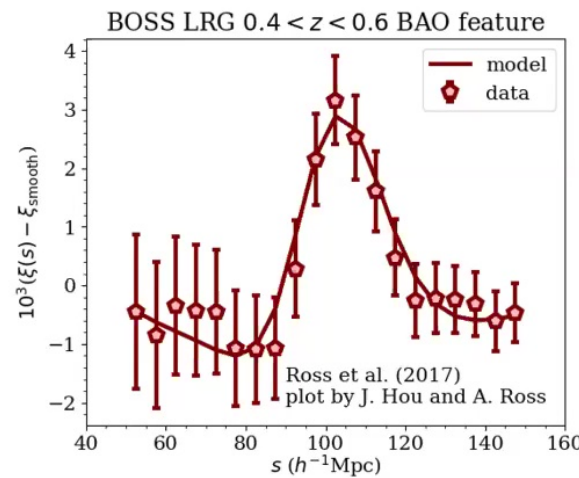
BAO from BOSS low-redshift bin ($0.2 < z < 0.5$)



Alam et al. (2017), MNRAS 470, 2617



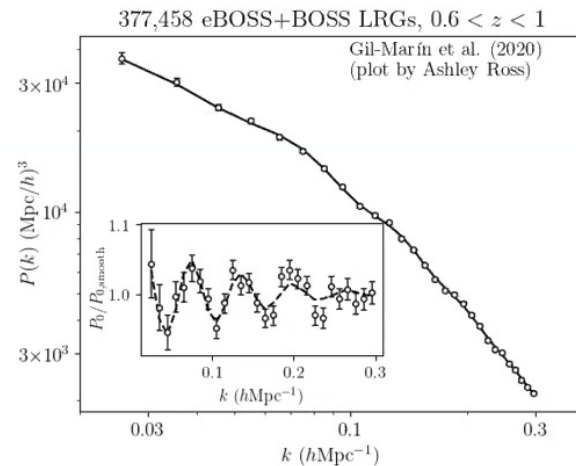
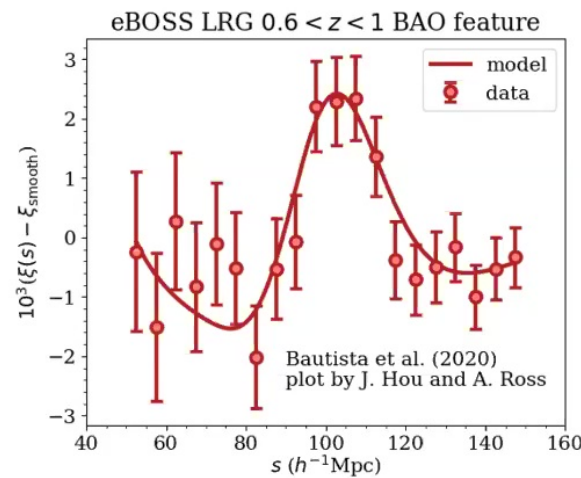
BAO from BOSS high-redshift bin ($0.4 < z < 0.6$)



Alam et al. (2017), MNRAS 470, 2617



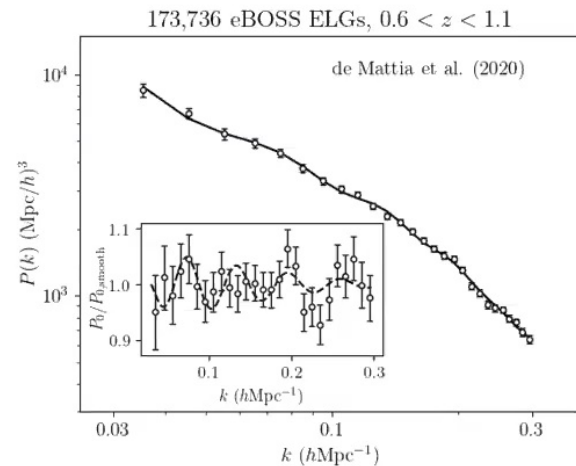
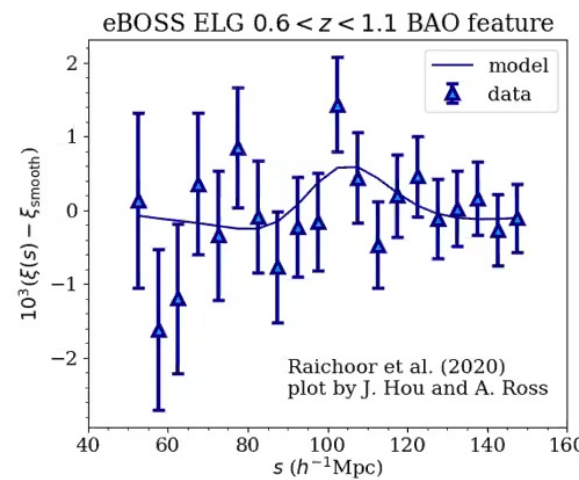
BAO from BOSS+eBOSS LRG ($0.6 < z < 1.0$)



Bautista et al. (2020), arXiv:2007.08993; Gil-Marín et al. (2020), arXiv:2020.08994



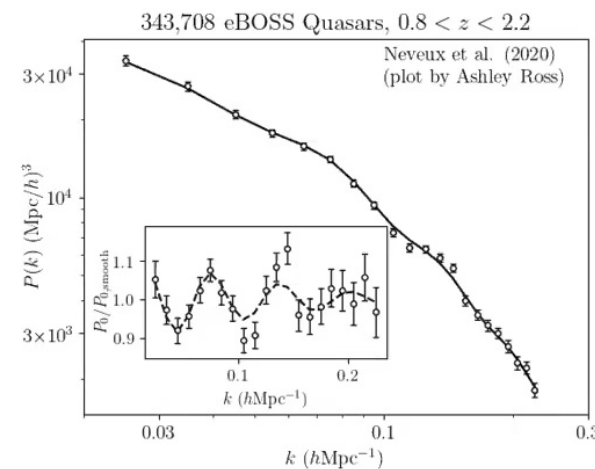
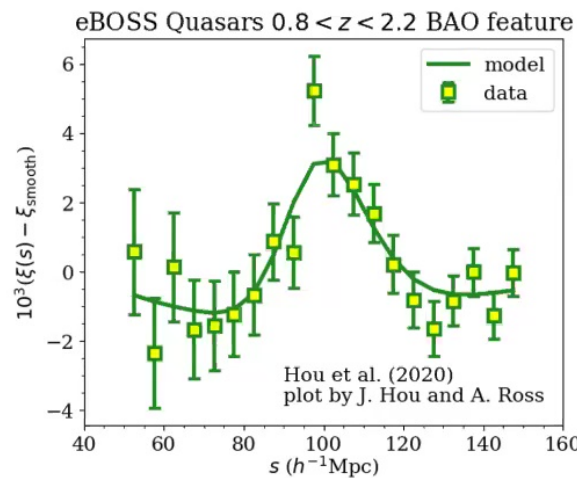
BAO from eBOSS ELG $0.6 < z < 1.1$



Raichoor et al. (2020), arXiv:2020.09007; de Mattia et al. (2020), arXiv:09008



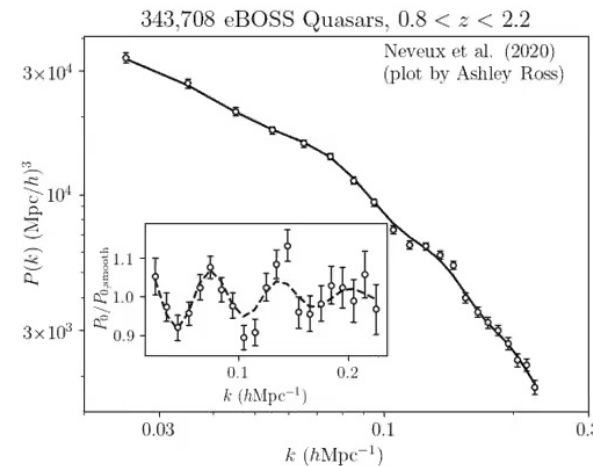
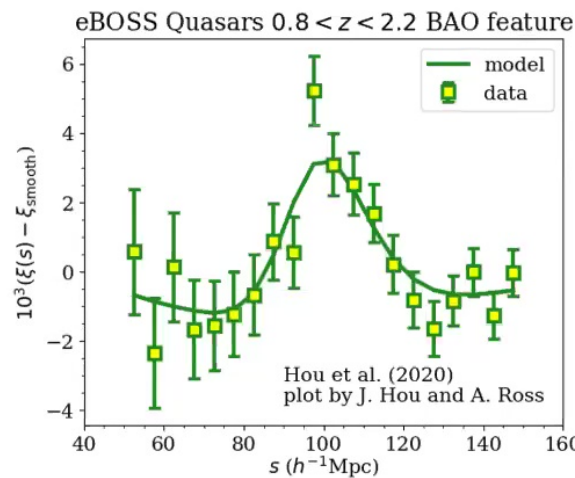
BAO from eBOSS QSO ($0.8 < z < 2.2$)



Hou et al. (2020), arXiv:2020.08998; Neveux et al. (2020), arXiv:08999



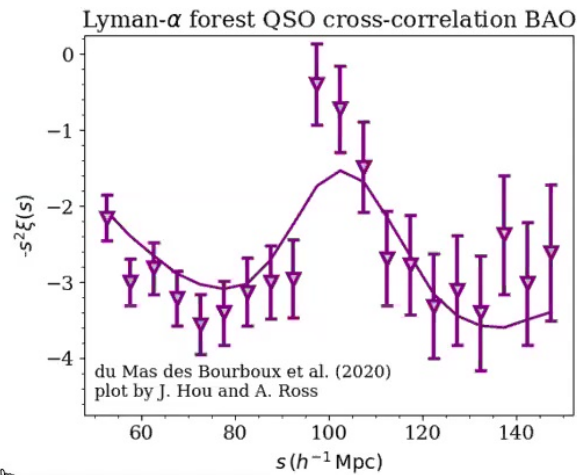
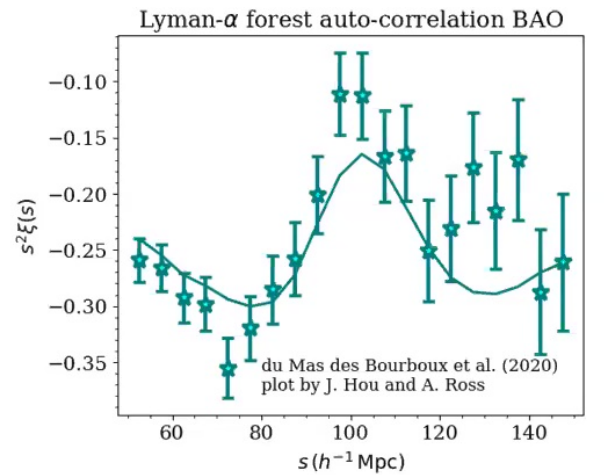
BAO from eBOSS QSO ($0.8 < z < 2.2$)



Hou et al. (2020), arXiv:2020.08998; Neveux et al. (2020), arXiv:08999



BAO from BOSS + eBOSS Ly- α

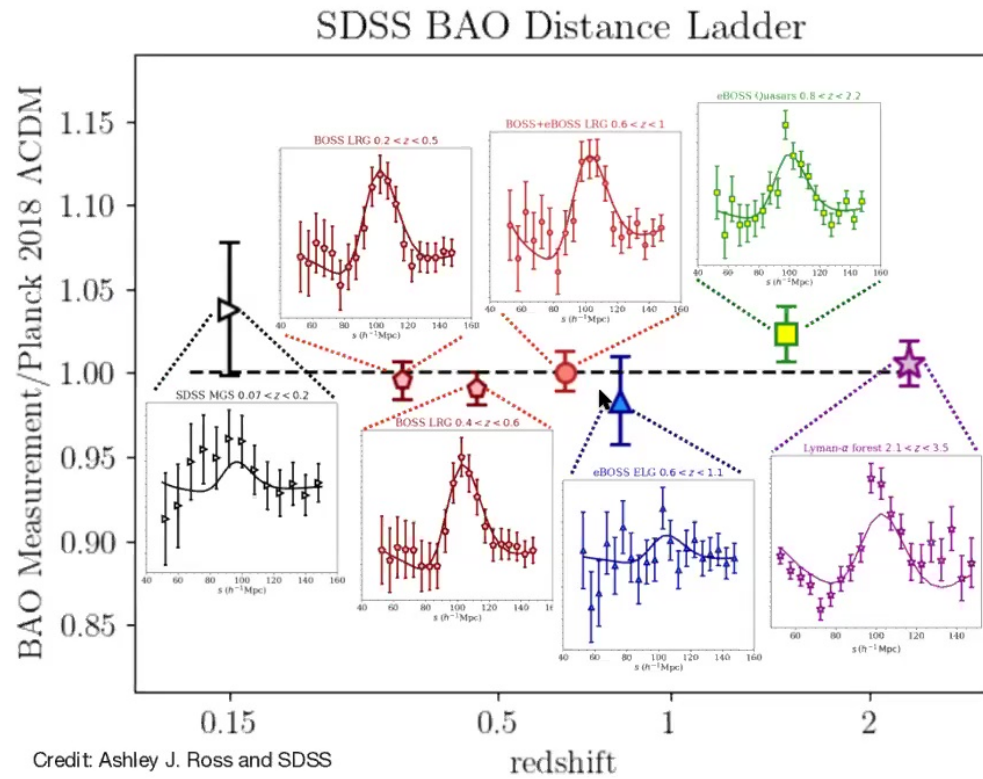


https://www.sdss.org/wp-content/uploads/
2020/07/xiw_lyaxcf_z_0_10_mu950.png

des Mas du Bourboux et al. (2020), arXiv:2020.08995

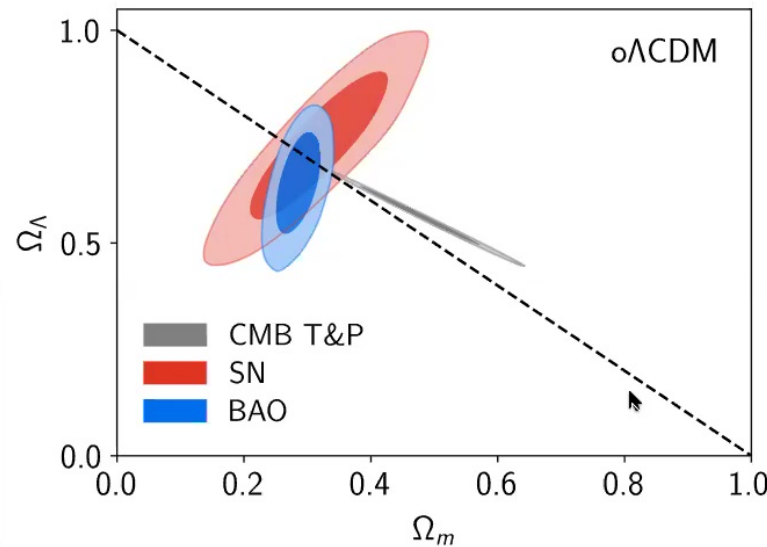


SDSS BAO Distance Ladder



WATERLOO CENTRE FOR
ASTRO
PHYSICS
UNIVERSITY OF WATERLOO

1. Detecting dark energy with BAO



Mueller et al. (2020), arXiv:2007.08991

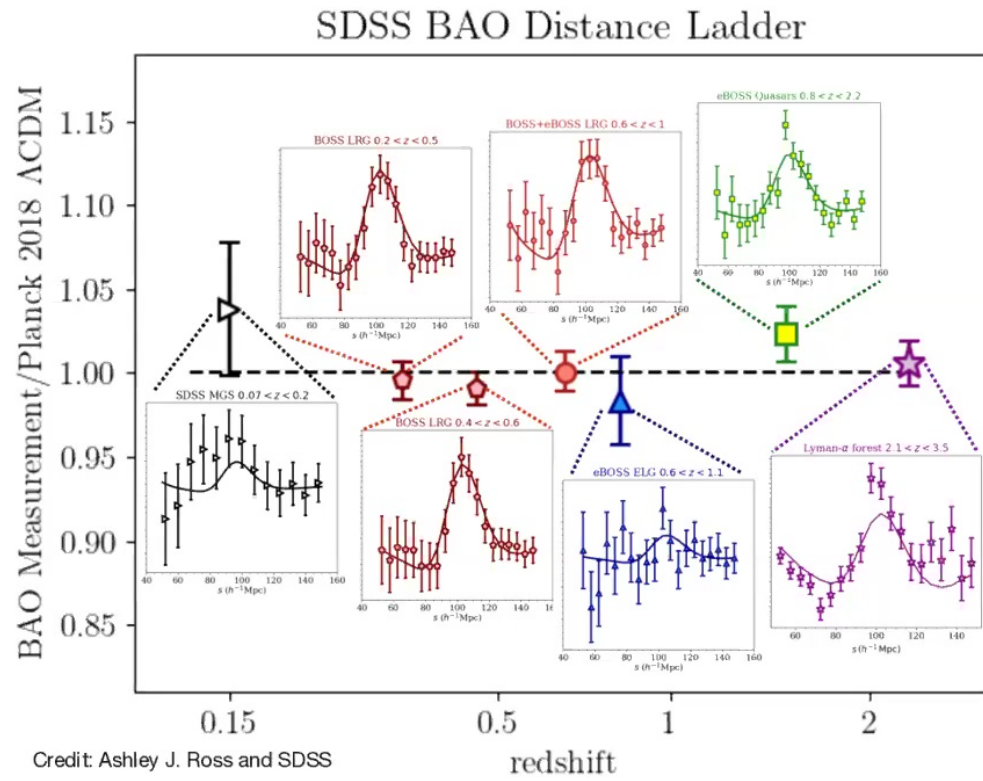
Constraints on the matter and dark energy components of the Universe while allowing for free curvature allow us to assess the impact of the SDSS BAO measurements. BAO measurements alone lead to a constraint on the dark energy density with an **8 σ confidence detection**.



SDSS BAO Distance Ladder



Will Percival

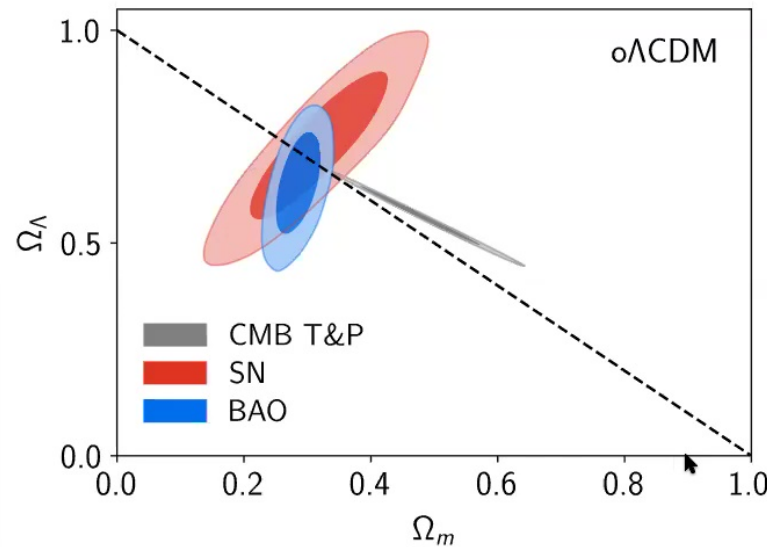


WATERLOO CENTRE FOR
ASTRO
 PHYSICS
UNIVERSITY OF WATERLOO

1. Detecting dark energy with BAO



Will Percival

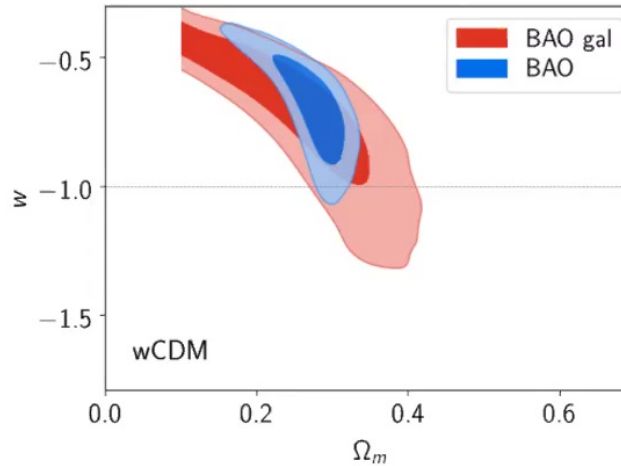
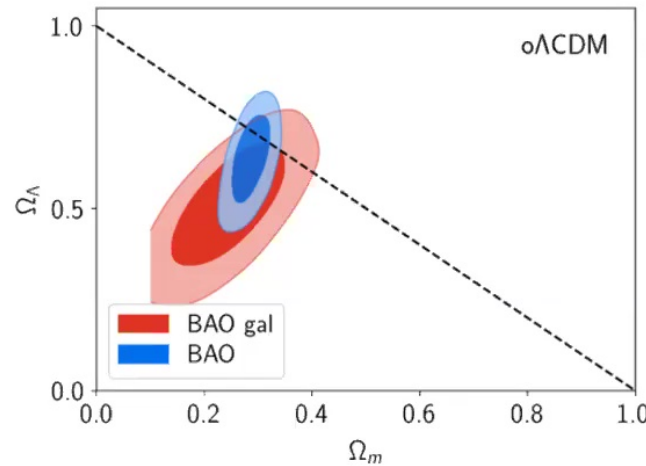


Mueller et al. (2020), arXiv:2007.08991

Constraints on the matter and dark energy components of the Universe while allowing for free curvature allow us to assess the impact of the SDSS BAO measurements. BAO measurements alone lead to a constraint on the dark energy density with an **8σ confidence detection.**



2. Low-z and high-z BAO



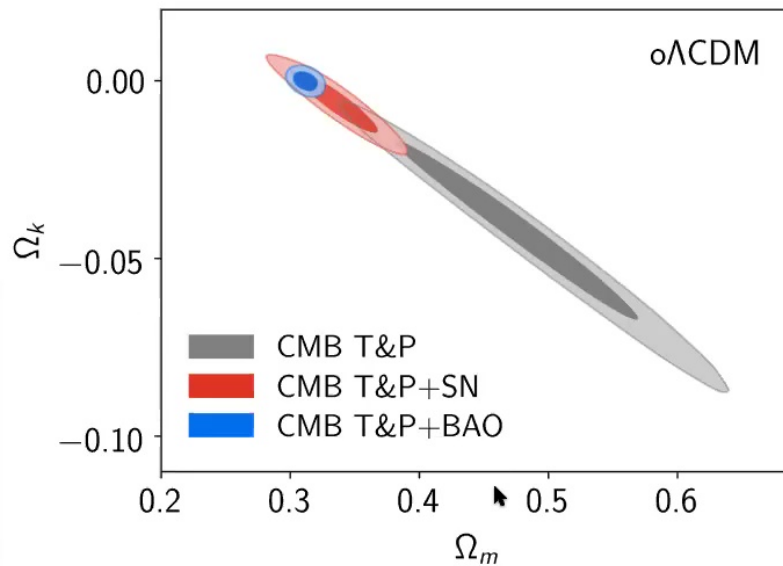
SDSS offer a unique combination of galaxy and quasar BAO at $z \leq 1.5$ along with the Lyman-alpha forest BAO at $z = 2.33$. With complementary degeneracy directions, low and high redshift measurements, when combined, allow precise constraints on both the matter density and the dark energy density.

Mueller et al. (2020), arXiv:2007.08991



Will Percival

3. The curvature of space from BAO

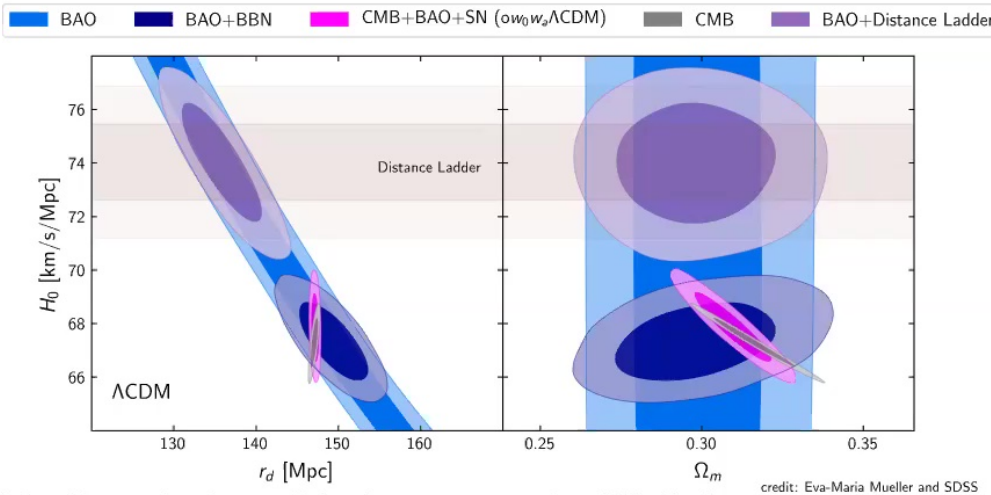


When combined with Planck temperature and polarization data, SDSS BAO measurements allow an order of magnitude improvement on curvature constraints compared to Planck data alone. The BAO data provide strong evidence for a nearly flat geometry and constraints on curvature that are now roughly one order of magnitude within the fundamental limits.

Mueller et al. (2020), arXiv:2007.08991



4. Local expansion history estimates



The BAO data allow robust, consistent measurements of H_0 that are insensitive to the strict cosmological priors in CMB-only estimates. BAO estimates are insensitive to the use of CMB anisotropies altogether under the assumption of a Λ CDM cosmology and including the Big Bang Nucleosynthesis constraints from primordial deuterium abundance. Under all assumptions, the H_0 values from BAO are roughly 10% smaller than those from the Cepheid distance ladder and strong-lensing time delays, and geometric distance to MASERs. The consistency of the BAO results highlights that the ‘ H_0 tension’ can not be restricted to systematic errors in Planck or to the strict assumptions of the Λ CDM model.

Mueller et al. (2020), arXiv:2007.08991





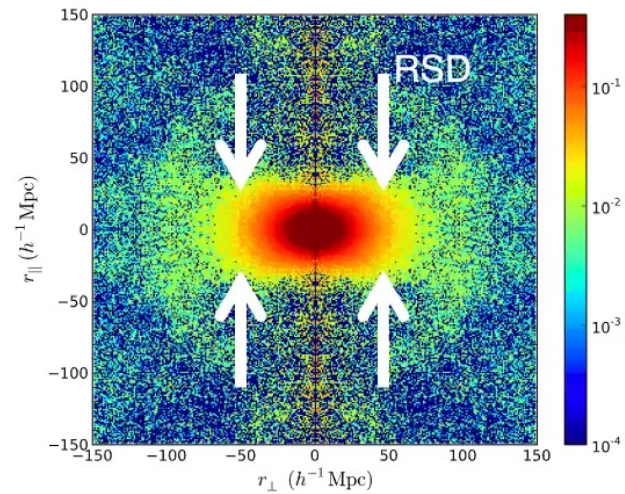
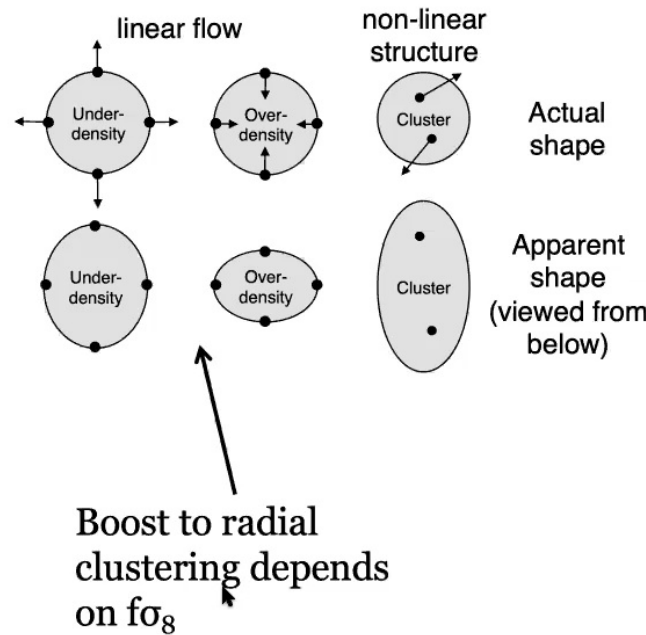
Redshift-Space Distortions





Will Percival

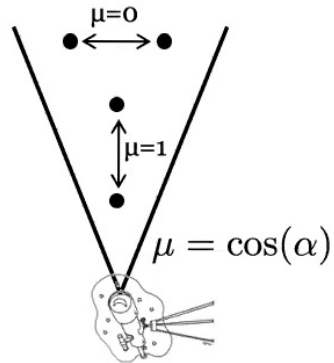
Redshift Space Distortions (RSD)



Samushia et al. 2013; MNRAS, 439, 3504;
Alam et al. 2016, arXiv:1607.03155



Moments of the clustering signal



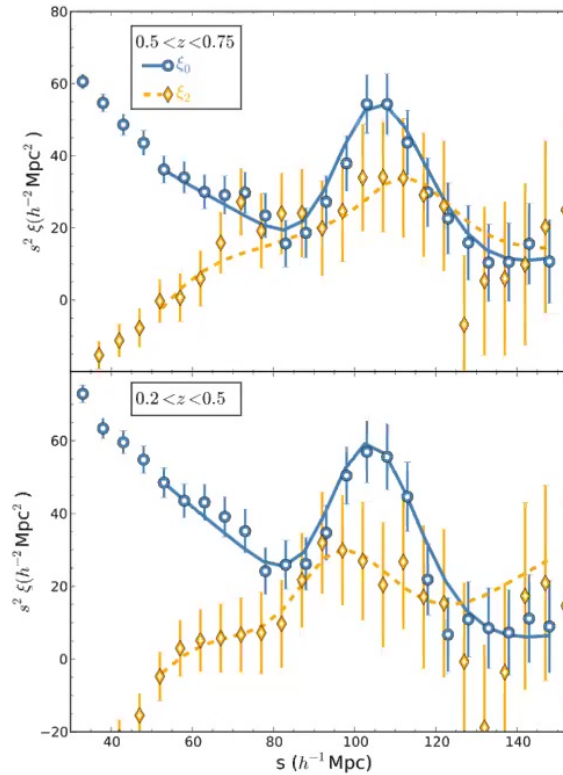
Define moments of the clustering signal

$$P_F(k) = \int_0^1 d\mu F(\mu) P(k, \mu)$$

$$\xi_F(r) = \int_0^1 d\mu F(\mu) \xi(r, \mu)$$

Monopole	$F(\mu)=1,$
Quadrupole	$F(\mu)=\frac{1}{2}(3\mu^2-1),$
Hexadecapole	$F(\mu)=\frac{1}{8}(35\mu^4-30\mu^2+3)$

RSD = non-zero quadrupole

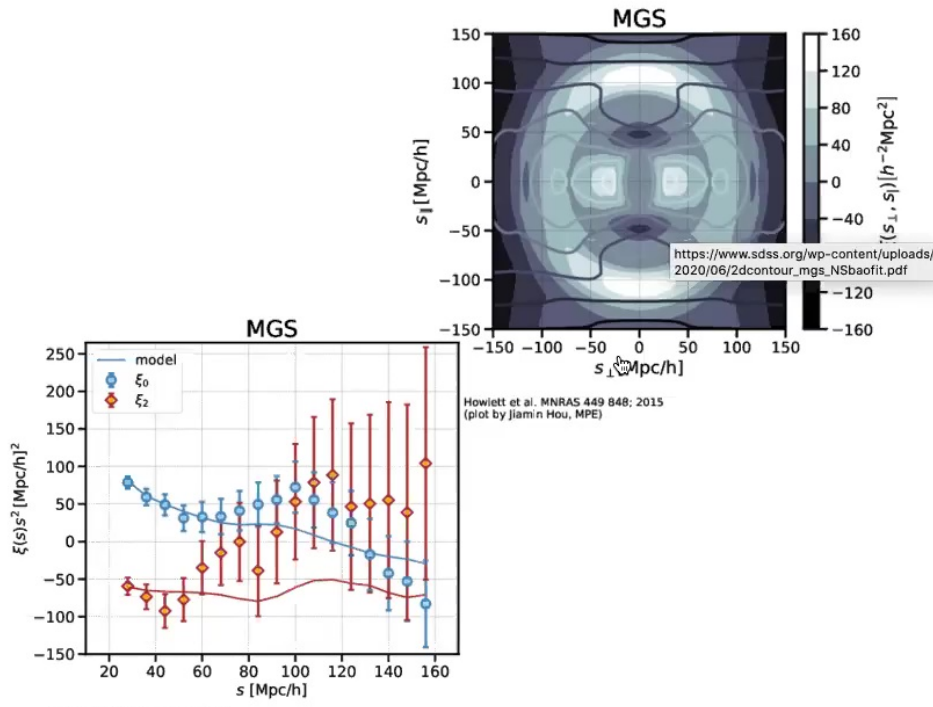


Ross et al. 2016, arXiv:1607.03145



Will Percival

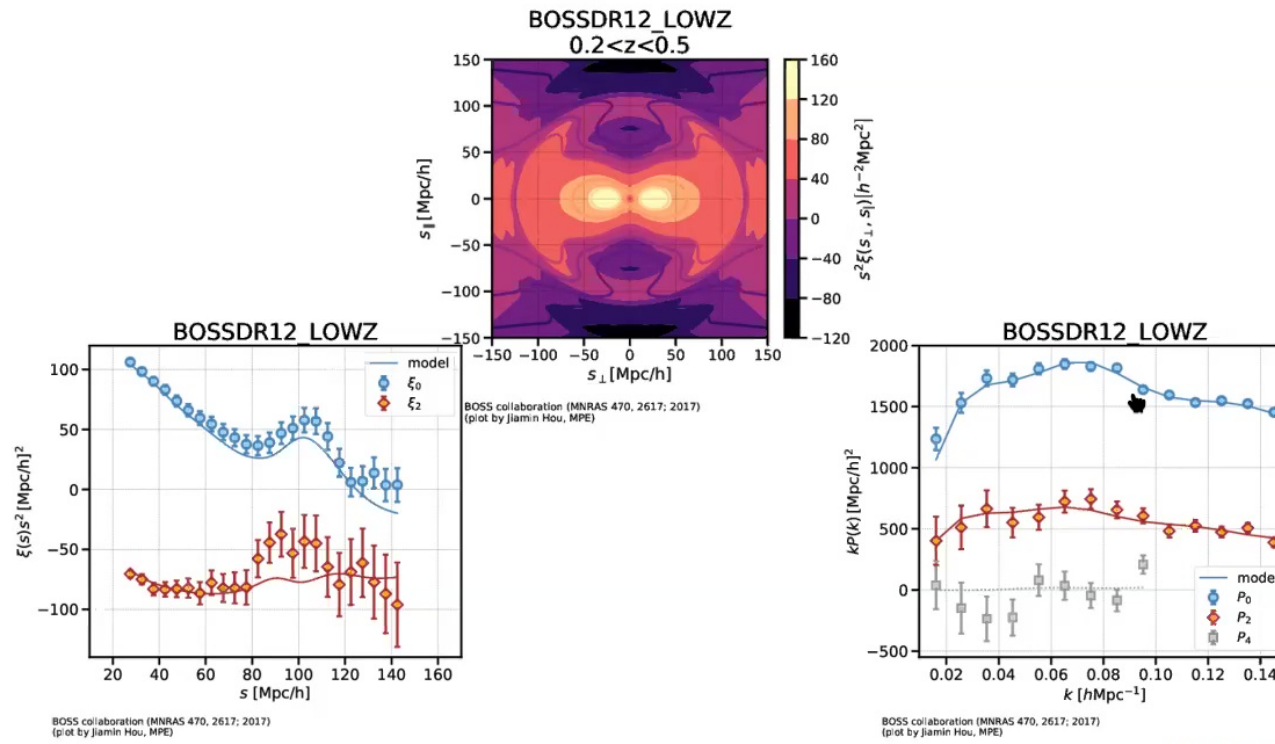
RSD from SDSS Main Galaxy Sample (0.07<z<0.2)



Howlett et al. (2015), MNRAS 449, 848



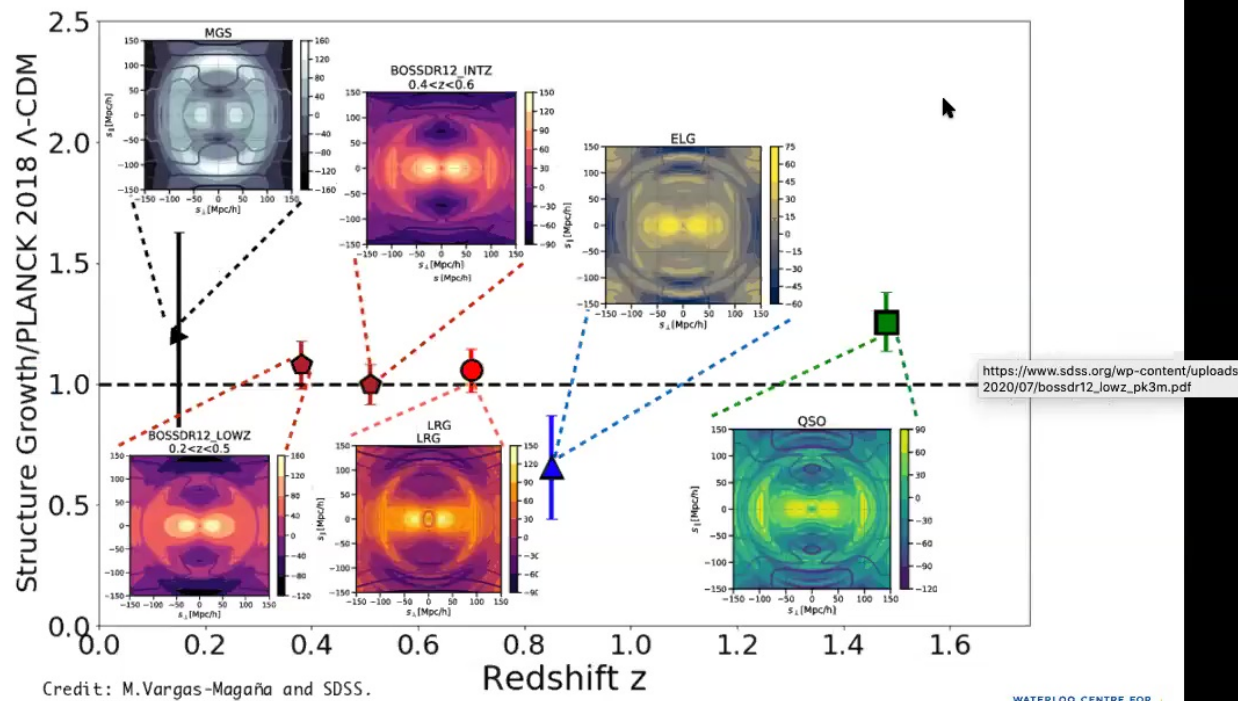
RSD from BOSS low-redshift bin ($0.2 < z < 0.5$)



Alam et al. (2017), MNRAS 470, 2617

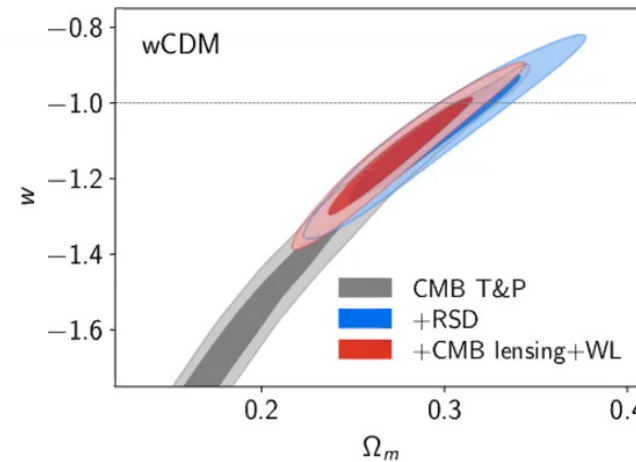
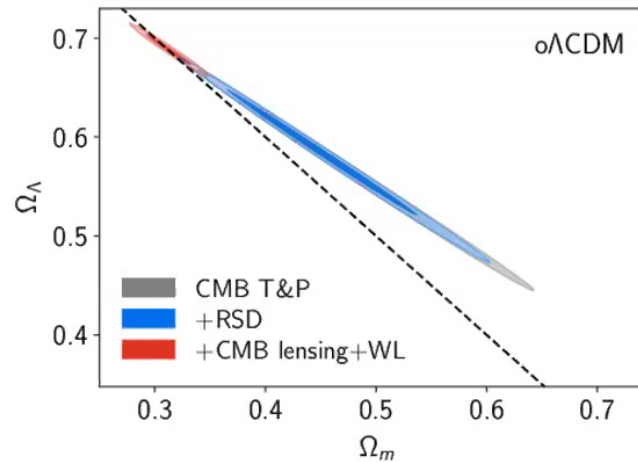


RSD measurements from SDSS



WATERLOO CENTRE FOR
ASTRO
 PHYSICS
UNIVERSITY OF WATERLOO

5. Dark Energy constraints from growth

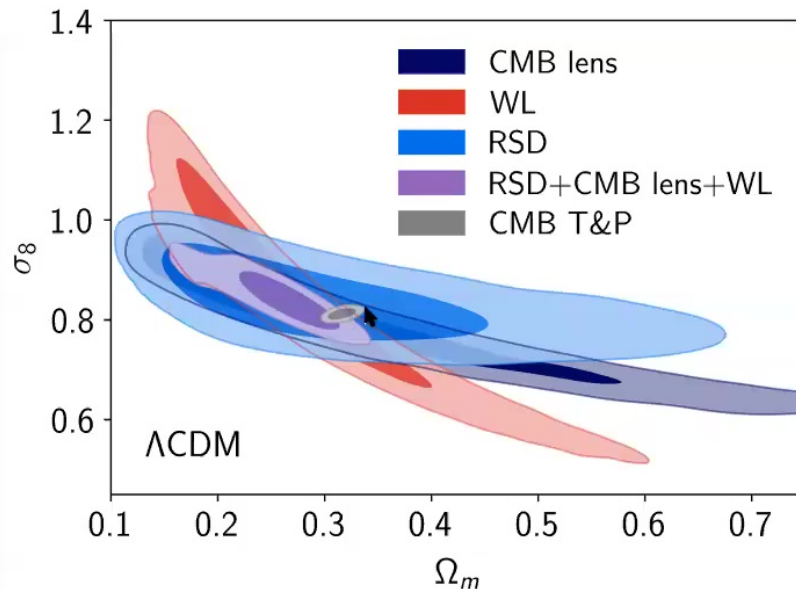


RSD growth measurements provide 2-3X improvements on the precision in extended ΛCDM models when compared to CMB temperature and polarization data alone. Weak lensing data instil a preference for a flat geometry while RSD instil a preference for a cosmological constant.

Mueller et al. (2020), arXiv:2007.08991



6. Consistency of General Relativity (GR) in predicting the rate of structure formation

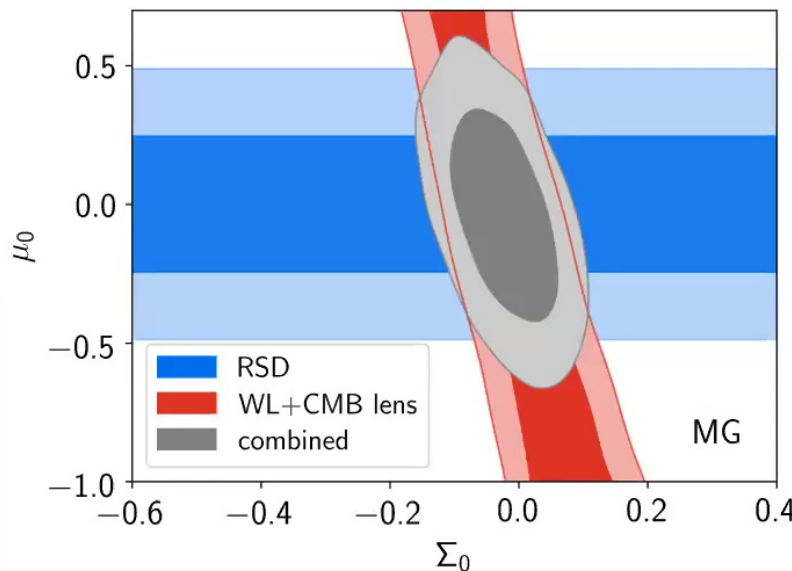


Mueller et al. (2020), arXiv:2007.08991

RSD and weak lensing allow us to estimate the current amplitude of matter fluctuations. We find a picture of structure growth that is consistent with extrapolations of the amplitude of the measured CMB power spectrum under a GR model for gravity and a Λ CDM model for cosmic expansion.



7. Testing GR predictions for matter and light



$$ds^2 = a^2(\tau)[(1 + 2\Psi)d\tau^2 - (1 - 2\Phi)\delta_{ij}dx_i dx_j]$$

$$k^2\Phi = -4\pi G a^2(1 + \mu(a))\rho\delta$$

$$k^2(\Psi + \Phi) = -8\pi G a^2(1 + \Sigma(a))\rho\delta$$

Mueller et al. (2020), arXiv:2007.08991

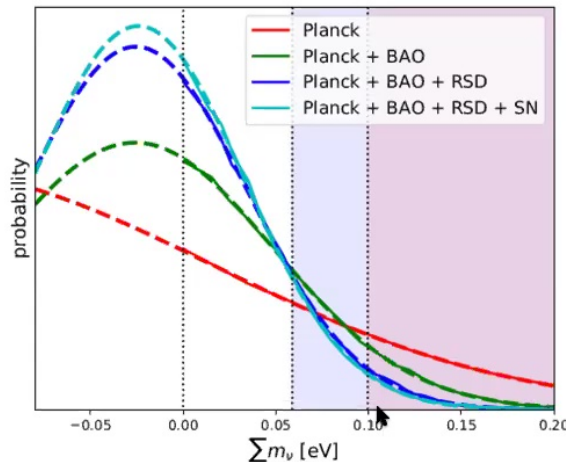
RSD measurements probe the gravitational response of matter while weak lensing measurements probe that of photons. These combined growth measurements provide evidence in support of the GR assumption that matter and photons follow the same interactions with a gravitational potential.



BAO + RSD



8. Bounds on neutrino mass



Data	95% upper limit [eV]	$P_{\text{inv}}/P_{\text{norm}}$	P_{unphy}	Gaussian fit [eV]
Planck	0.252	0.64	0.43	
Planck + BAO	0.129	0.36	0.64	-0.026 ± 0.074
Planck + BAO + RSD	0.102	0.24	0.76	-0.026 ± 0.060
Planck + SN	0.170	0.49	0.56	-0.076 ± 0.106
Planck + BAO + RSD + SN	0.099	0.22	0.78	-0.024 ± 0.057
Planck + BAO + RSD + SN + DES	0.111	0.27	0.71	-0.014 ± 0.061
Planck + BAO + RSD + SN (νw CDM)	0.139	0.40	0.61	-0.033 ± 0.082
Planck + BAO + RSD + SN + DES (νw CDM)	0.161	0.48	0.56	-0.048 ± 0.097

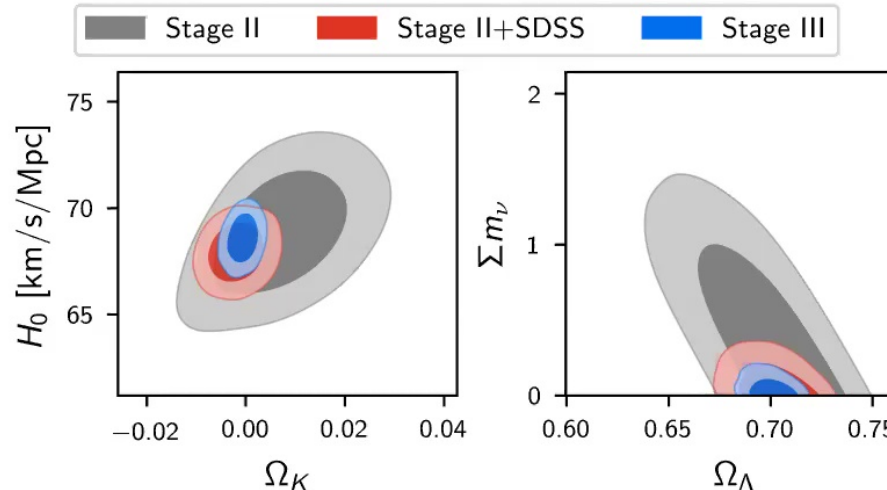
Mueller et al. (2020), arXiv:2007.08991

The combined analysis allows very tight constraints on the summed mass of the three neutrino species, with an uncertainty that is almost equal to the lower bound of 60 meV allowed by neutrino oscillation experiments. Using the Planck data as a baseline, the largest improvement in precision comes from the addition of the SDSS BAO measurements, while the RSD improve the precision by another 23%.



Will Percival

9. Role of SDSS in cosmology over the last decade

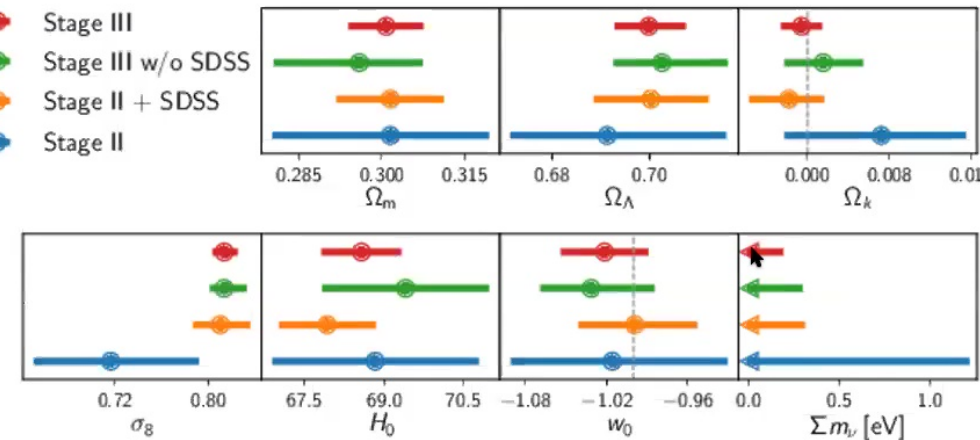


Model with free curvature, neutrino mass, and constant equation of state for dark energy.
 Stage-II: WMAP, JLA Supernovae, and low redshift measurements of the baryon acoustic oscillations. The posterior volume spanned by w , curvature (Ω_k), H_0 , fluctuation amplitude (σ_8), and neutrino mass decreases by a factor of 40 when adding the SDSS BAO and RSD data to Stage-II experiments. The biggest impact from SDSS is in improved constraints on Ω_k , H_0 , and neutrino mass. The volume decreases by another factor of 25 when adding Planck, Pantheon SNe Ia, and DES data, for a total improvement of three orders of magnitude in the precision in this 5D parameter space.

Mueller et al. (2020), arXiv:2007.08991



9. Role of SDSS in cosmology over the last decade

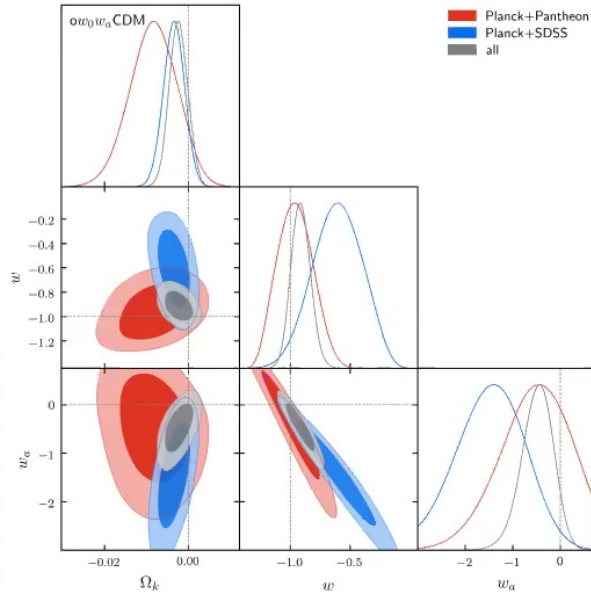


Model with free curvature, neutrino mass, and constant equation of state for dark energy. Stage-II: WMAP, JLA Supernovae, and low redshift measurements of the baryon acoustic oscillations. The posterior volume spanned by w , curvature (Ω_k), H_0 , fluctuation amplitude (σ_8), and neutrino mass decreases by a factor of 40 when adding the SDSS BAO and RSD data to Stage-II experiments. The biggest impact from SDSS is in improved constraints on Ω_k , H_0 , and neutrino mass. The volume decreases by another factor of 25 when adding Planck, Pantheon SNe Ia, and DES data, for a total improvement of three orders of magnitude in the precision in this 5D parameter space.

Mueller et al. (2020), arXiv:2007.08991



10. Summary cosmological model



The tightest constraints on the cosmological model are found when combining current measurements of the expansion history, CMB, and growth of structure. This combination reveals a dark energy density measured to 0.7% precision under an assumed Λ CDM model. We find $\sim 1\%$ precision estimates on the dark energy density (Ω_Λ), H_0 , and σ_8 regardless of cosmological model, with a preference for a cosmological constant and a flat Universe under all models explored. The complementarity of BAO and SNe Ia data allow tight constraints of curvature and the dark energy equation of state, resulting in a Dark Energy Task Force Figure of Merit of 92.

Mueller et al. (2020), arXiv:2007.08991



Will Percival

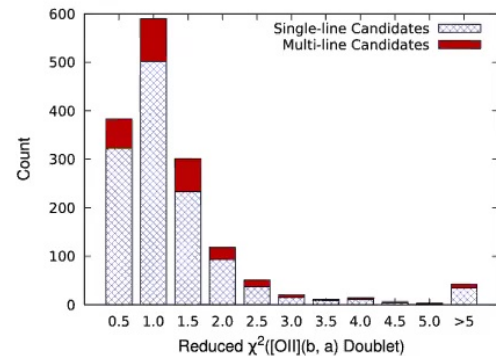


Will Percival

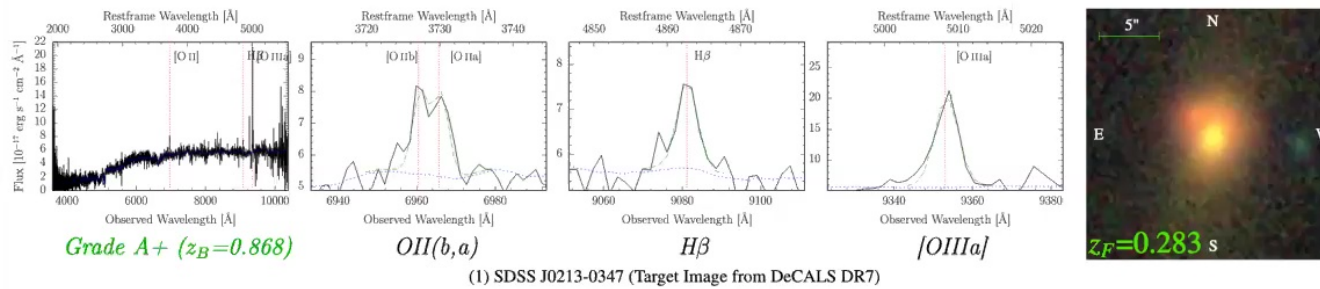
Other measurements



Strong lens catalog



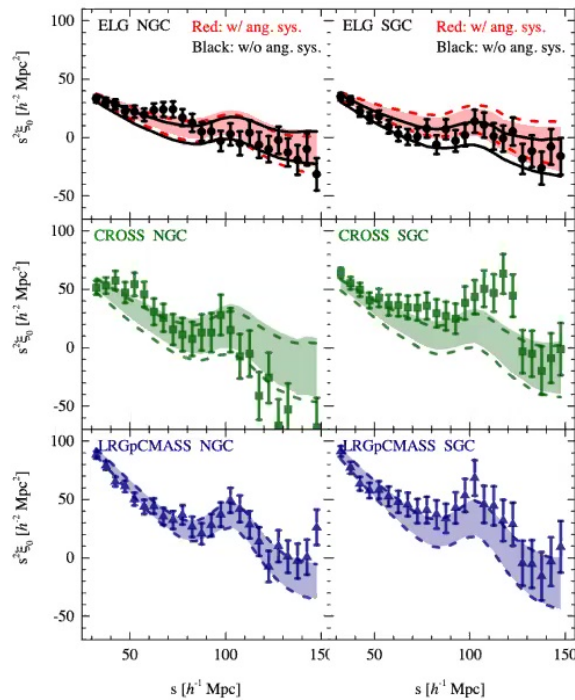
Looked for strong lens candidates by subtracting galaxy model from spectrum and looking for background emission lines: 838 likely, 448 probably, 265 possible



Talbot et al. (2020), arXiv:2007.09006



Multi-tracer analyses



Use angular overlap between ELG and LRG samples to make “sample variance-free” measurements of ratios:
18% improvement on $f\sigma_8$.

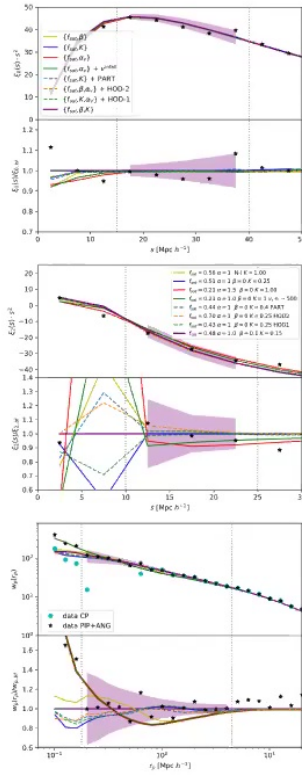
Samples	α_{\perp}	α_{\parallel}	$f\sigma_8$	χ^2/dof
ELG	$1.097^{+0.374}_{-0.236}$	$1.173^{+0.248}_{-0.219}$	$0.432^{+0.135}_{-0.149}$	169/138
ELG, SGC	$1.033^{+0.071}_{-0.130}$	$1.127^{+0.095}_{-0.163}$	$0.431^{+0.104}_{-0.132}$	92/67
ELG	fixed	fixed	0.433 ± 0.045	169/140
LRGpCMASS	1.016 ± 0.021	1.007 ± 0.028	0.472 ± 0.043	161/138
LRGpCMASS	fixed	fixed	0.448 ± 0.032	161/140
CROSS	0.949 ± 0.040	1.118 ± 0.118	0.342 ± 0.085	147/138
CROSS	fixed	fixed	0.443 ± 0.050	148/140
ELG+LRGpCMASS	1.004 ± 0.020	1.020 ± 0.028	0.435 ± 0.037	309/279
ELG, SGC + LRGpCMASS	1.013 ± 0.021	1.014 ± 0.028	0.451 ± 0.041	232/208
ELG+CROSS	0.970 ± 0.037	1.044 ± 0.072	0.402 ± 0.062	290/279
CROSS+LRGpCMASS	1.006 ± 0.021	1.016 ± 0.029	0.444 ± 0.041	298/279
Joint ($N_p = 10$)	1.003 ± 0.020	1.018 ± 0.030	0.439 ± 0.039	416/422
Joint ($N_p = 10$, w/ AP fixed)	fixed	fixed	0.444 ± 0.029	414/424
Joint ($N_p = 12$)	1.005 ± 0.020	1.016 ± 0.028	0.445 ± 0.038	416/420
Joint ($N_p = 12$, w/ AP fixed)	fixed	fixed	0.446 ± 0.029	414/422

Wang et al. (2020), arXiv:2007.09010, Zhao et al. (2020), arXiv:2007.09011 (similar with $P(k)$)

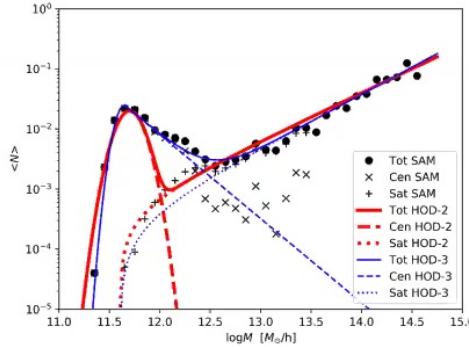


Will Percival

ELG HOD



Avila et al. (2020), arXiv:2007.09012



ELGs trace halos in a complicated way (compared to LRGs) as they have more satellites and hence a more complicated HOD. This project fits models to the data, including small-scales using PIP weights.

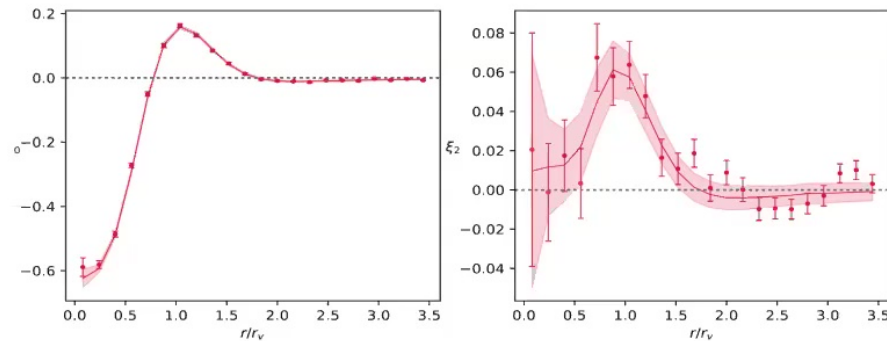
Mock	HOD	<i>f</i> _{sat}	β	K	α_V	profile	v_{infall}	χ^2_{wp}	χ^2_2	χ^2_0	χ^2_{tot} (bins: 14+3+5)
0	HOD-3	0.22	0	1	1	NFW	0	21.7	1.1	5.0	31.3
1	HOD-3	0.56	N-I	1	1	NFW	0	17	0.3	4.7	24
2	HOD-3	0.51	0	0.25	1	NFW	0	7.2	0.3	5	12.7
3	HOD-3	0.21	0	1	1.5	NFW	0	22	0.5	5.3	28.3
4	HOD-3	0.21	0	1	1.0	NFW	-500	22	0.5	5.0	28
5	HOD-3	0.36	0.0	1	1	PART	0	15.5	0.7	4.7	23
6	HOD-3	0.44	0	0.4	1	PART	0	8	0.3	4.6	13.5
7	HOD-3	0.26	0	1	1.2	PART	0	15	0.2	4.6	21.4
8	HOD-3	0.26	0	1	0.8	PART	-500	16	0.9	4.3	21.2
9	HOD-3	0.48	0.10	0.15	1	NFW	0	6	0.3	4.9	10.9
10	HOD-3	0.21	0.0	1	1.5	NFW	0	22	0.5	5.3	28.3
11	HOD-3	0.51	0	0.25	1.0	NFW	0	7.2	0.3	5	12.7
12	HOD-1	0.40	N-I	1	1	NFW	0	17.9	0.3	4.7	25
13	HOD-1	0.43	0	0.25	1	NFW	0	7	0.3	5.0	12.4
14	HOD-1	0.18	0	1	1.6	NFW	0	22	0.3	5.5	28.6
15	HOD-2	0.70	N-I	1	1	NFW	0	21	0.3	4.9	28.4
16	HOD-2	0.70	0	0.25	1	NFW	0	8.1	0.3	4.8	13.8
17	HOD-2	0.22	0	1	1.5	NFW	0	22	0.2	5.4	29.1



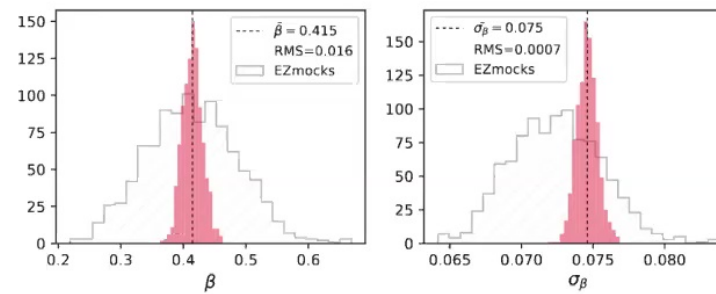
Will Percival



Voids



Simple RSD
measurements from
the growth of voids.



Aubert et al. (2020), arXiv:2007.09013



Will Percival



Discussion

- Still to come
 - f_{NL} analyses from large-scale clustering of QSOs
 - RSD + AP void analyses (draft in review)
 - Small-scale RSD measurements
 - More cosmological tests (for example E_G statistic draft in review)
- Resources
 - <https://www.sdss.org/science/final-bao-and-rsd-measurements/>
 - <https://www.sdss.org/science/cosmology-results-from-eboss/>
 - <https://arxiv.org/abs/2007.08991> ... <https://arxiv.org/abs/2007.09013>



Will Percival

